INVESTIGATION OF STRUCTURAL AND OPTICAL PROPERTIES OF PURE SNO_2, ZNO AND SNO_2/ZNO COMPOSITE NANORODS

A Dissertation

SUBMITTED IN PARTIAL FULFILMENT OF THE REQUIREMENT

FOR THE AWARD OF THE DEGREE

OF

MASTER OF SCIENCE

IN

APPLIED PHYSICS

Submitted by

Vineeta yadav 2K20/MSCPHY/36

Nirmal 2K20/MSCPHY/19

Under the supervision of

Dr. Deshraj Meena

Department of Applied Physics

Delhi Technological University

Bawana Road, Delhi -110042

MAY 2022

CANDIDATE'S DECLARATION

We hereby certify that the work which is presented in the Major Project-Il/Research Work entitled in fulfilment of the requirement for the award of the Degree of Mastes of Applied Physics in and submitted to the Department of Applied Physics Delhi Technological University, Delhi is an authentic record of my/our own, carried out during a period from sAugust 2021 to May 2022 under the supervision of Dr. Deshraj Meena.

The matter presented in this report/thesis has not been submitted by us/me for the award of any other degree of this or any other Institute/University. The work has been published/accepted/communicated in SCI/ SCI expanded/SSCI/Scopus indexed journal OR peer reviewed Scopus indexed conference with the following details

Title of Paper: "Investigation of structural and optical properties of pure SnO_2, ZnO and SnO_2/ZnO composite nanorods"

Authors: Vineeta Yadav, Nirmal Singh, Deshraj Meena

Conference:13th International Conference on Material Processing and Characterization (ICMPC) -2022 (Published in Materials Today Proceedings)

Confrence Date: 22-24 April 2022

Submitted on: 31th MARCH, 2022

Accepted on: 8thAPRIL, 2022
Publication Date: 22nd April 2022

VINEETA YADAV, NIRMAL
2K20/MSCPHY/36, 2K20/MSCPHY/19
M.Sc., Applied Physics

SUPERVISOR CERTIFICATE

To the best of my knowledge, the report comprises original work. It has not been submitted in part or whole for any Course/Degree to this university or elsewhere as per the candidate's declaration.

Place: Delhi

Date:10 MAY 2022

Dr. DESHRAJ MEENA

Acknowledgment

We feel immense pleasure in expressing our deep gratitude and an overwhelming sense of pride towards our guide, Dr.Deshraj Meena whose constant help and support, complete involvement, invaluable guidance and encouragement, and critical analysis of our result, led us to complete this project and gain preliminary knowledge of research. We owe our sincere thanks to him for allowing us to work under his guidance.

We would like to express our deepest appreciation to Ms. Shilpa Rana for her support, continuous guidance in laboratory work and research during the project. Also, we express our heartfelt gratitude to Ms. Komal who helped us along the way in our project.

We would also like to take this opportunity to thank the HOD of the Department of Applied Physics, Dr. Rinku Sharma for overlooking and enabling us to use all the facilities that were required and for going out of her way to help students in any matter.

Without the help of the aforementioned individuals, the project would not have been as easily carried out, we would have faced many difficulties throughout the project.

Vineeta Yadav (2K20/MSCPHY/36) Nirmal (2K20/MSCPHY/19

REGISTRATION RECORD

Materials Today Proceedings <em@editorialmanager.com> Thu, Mar 31, 12:09 AM
to me

Dear Ms. Yadav,

Thank you for registering for the Editorial Manager online submission and peer review tracking system for Materials Today: Proceedings.

Here is your username, which you need to access Editorial Manager at https://www.editorialmanager.com/matpr/.
Username: Vineeta Yadav

If you do not know your confidential password, you may reset it by clicking this link: https://www.editorialmanager.com/matpr/l.asp?i=540758&l=AFM5YPF0

Please save this information in a safe place.

You can change your password and other personal information by logging into the Materials Today: Proceedings website and clicking on the Update My Information link on the menu.

Best regards,
Materials Today: Proceedings

For more information on using EM, please refer to Aries Systems' user Tutorials and Video Library:
https://www.ariessys.com/for-current-customers/tutorials/
https://www.ariessys.com/views-and-press/resources/video-library/
You can also access these videos by clicking the "Play" icon in the top right corner of the EM site.

ACCEPTANCE RECORD

Editor Decision - Accept on your article MATPR-D-22-02949 External Inbox ×

Swadesh Kumar Singh <em@editorialmanager.com> Fri, Apr 8, 1:19 PM
to me

Ms. Ref. No.: MATPR-D-22-02949
Title: Investigation of structural and optical properties of pure SnO2, ZnO and SnO2/ZnO composite nanorods
Materials Today: Proceedings

Dear Ms. Vineeta Yadav,

I am pleased to inform you that your paper "Investigation of structural and optical properties of pure SnO2, ZnO and SnO2/ZnO composite nanorods" has been accepted for publication in Materials Today: Proceedings.

Below are comments from the editor and reviewers.

Thank you for submitting your work to Materials Today: Proceedings.

Yours sincerely,

Swadesh Kumar Singh, Ph.D.
Managing Guest Editor
Materials Today: Proceedings

Comments from the editors and reviewers:

Certificate

Certificate

of Participation

This certificate is awarded to Prof./Dr./Mr./Ms **Vineeta Yadav** for participating and presenting a paper titled ***Investigation of structural and optical properties of pure SnO2, ZnO and SnO2/ZnO composite nanorods*** in 13th International Conference on Material Processing and Characterization (ICMPC-2022) conducted by the Department of Mechanical Engineering, Gokaraju Rangaraju Institute of Engineering and Technology Hyderabad, India during 22-24 April 2022.

Convenor	HOD	Principal
Prof. Swadesh Kumar Singh	Dr, B. Tanya	Dr. J. Praveen
GRIET, Hyderabad	GRIET, Hyderabad	GRIET, Hyderabad

Fee Receipt

SBI

IMPS Transaction Detail

Reference No.	IMPS00198941806
Debit Account Number	00000034036663624
Credit Account Number	916010080365885
Transaction Date	07-Apr-2022
Amount	INR 9,000.00
Status	Success
Reason	Processed

Contents

List of Figures

List of Tables

List of symbols and abbreviations

S.no.	List of Symbols	
	Symbol	Full Form
1.	SnO_2	Tin Oxide
2.	WH Plot	Willianson Hall Plot
3.	$SnCl_4.5H_2O$	Tin Tetrachloride
4.	$ZnCl_2$	Zinc Chloride
5.	$ZnSO4.7H_2O$	Zinc Sulphate Heptahydrate
6.	$ZnCl_2$	Zinc Chloride
7.	KOH	Potassium Hydroxide
8.	Na_2CO_3	Sodium Carbonate

Abbreviations:

S.no.	Abbreviations
1.	3D = Three dimensional
2.	NWS=Nanowires
3.	NRS=Nanorods
4.	XRD=X Ray Diffraction

5.	$ZnCl_2$=Zinc Chloride
6.	DI=De-ionized water
7.	SMO=Semiconductor Metal Oxide

Abstract

Nanorods of SnO_2, ZnO and SnO_2/ZnO composites were successfully synthesised by the hydrothermal method in a one step process under specific conditions. The lattice strain and crystallite size of the nanorods were calculated using Williamson-Hall and Scherrer methods. TEM (Transmission Electron Microscopy) results confirm the synthesized samples are nanorods. The various crystalline planes of the nanorods were also identified using SAED (Selected Area Electron Diffraction) Pattern. The EDS (energy dispersive spectroscopy) result confirms the chemical purity of the nanorods. Furthermore, the optical band gap of SnO_2/ZnO nanocomposite was found to be lesser than the pure optical bandgaps of both SnO_2 and ZnO nanorods. Various functional groups were found to be on the surface of the synthesized nanorods, from the FTIR analysis.

CHAPTER 1

1. Introduction

In recent years, many applications, including [1] gas sensors [2], solar cells [3], lithium-ion batteries (LIBs)[3], and other opto-electronic nanodevices [6–9] are studied for metal oxide nano-wires, nano-tubes and nanofibers (Semi-conductor nanostructures), due to their appreciable electronic structural characteristics, optical properties and various chemical properties. The metal oxides that are formed between metal cations and oxide ions are the chemical compound. Moreover, due to their band gaps being wide and exciton binding energy being high, ZnO, TiO_2, SnO_2, CuO, Fe_2O_3 etc, are earlier reported to be some of best holders of semiconducting properties in metal oxides due to their wide band gap and high exciton binding energy. In ii and iv group of semiconductors Zn and Sn have attracted a lot of researchers due to their unique properties like band gap of 3.37 eV and also large exciton binding energy (60 Mev). Tin dioxide (SnO_2) and Zinc oxide (ZnO) have been widely used as photocatalyst for photodegradation of organic compounds, sensing material in resistive gas sensors, perovskite solar cells, liquid crystal display, biosensors, acoustic photodevices and photodiodes, electrochemical supercapacitors, catalysts and in the development of electrode materials for LIBs [3]. Both of these metal oxides have high melting point and large cohesive energy, excellent thermal and mechanical stability, good electrical conductivity, and high transparency in the visible spectrum. These properties make them obvious for the above application. Moreover, both are easily available and environment friendly. It has been observed that to obtain the desired materials with enhanced properties, the nanostructures of SnO_2 and ZnO composite has been used in many applications [4-5 both are easily available and environment friendly. The efficiency for the devices based on pure metals are lower than the devices based on SnO2/ZnO nanocomposites as reported in previous literature [6]. Composites are advantageous as they have been found more porous in comparison with the pure metal oxides. Especially, SnO_2 can be made porous with the addition of ZnO in very small amounts [6].

In the present work, a comparative analysis of the structural and optical properties of SnO_2/ZnO nanocomposites with pure SnO_2 and ZnO has been done. The nanorods of the pure SnO_2, ZnO and SnO_2/ZnO composites were synthesized using hydrothermal method. The results reveal that the composites have lower optical band gap in comparison with pure SnO_2 and ZnO. The

efficiency of charge separation is greatly improved by threshold energy difference of SnO_2 and ZnO, thus improving the optical properties.

CHAPTER 2

2. Litrature review

2.1 Paper 1

One-step synthesis of scions SnO2/ZnO heterostructures and their improved gas sensing properties

This paper studied about branch heterostructure composite of the nanorods of zinc oxide which were backbones and the tin oxide were as a branch was prepared using the facile one-step hydrothermal method and the morphology and structure of the components of these composites were characterized by the SEM and x-ray powder diffraction and elemental mapping analysis the evolution process of the composites were observed by the SEM and it was studied the composites with the novel hydro structures were fabricated for a good sensor and other gases in properties were tested for various gases like ethanol methanol and acetone ammonia two words which give which gave different responses from 18 to 100 PPM.

Results

In the paper branched SnO_2 heterostructures were composed of ZnO on which SnO2 wwas loaded by hydrothermal method.The structural and morphological properties were studied for this novel structure.Gas sensors were fabricated using this sample and gas sensi parameters were studied.It was found that the the composites exhibited thebetter gas sensing properties .The reason for the better performance may be beacause of the formation of the N-N heterostructure which increased the resistance of the sensor compared pure zinc oxide sample .

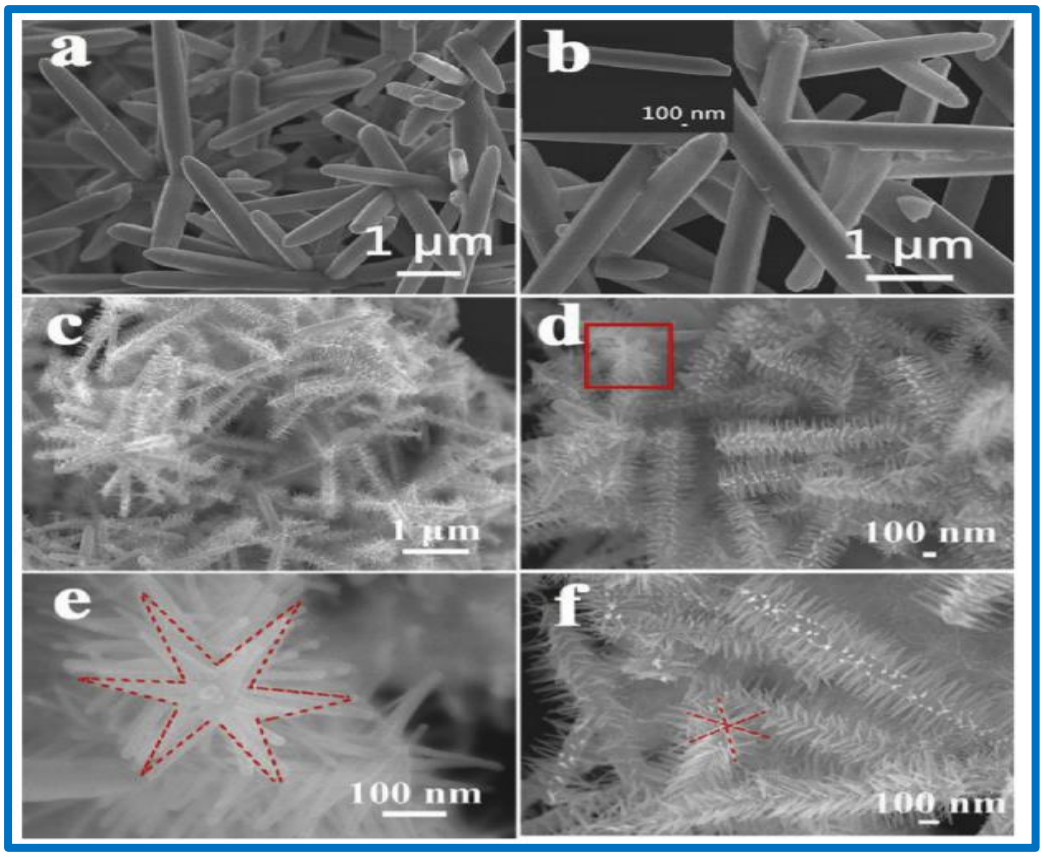

Figure 1 SEM images of the SnO_2/ZnO heterostructure.

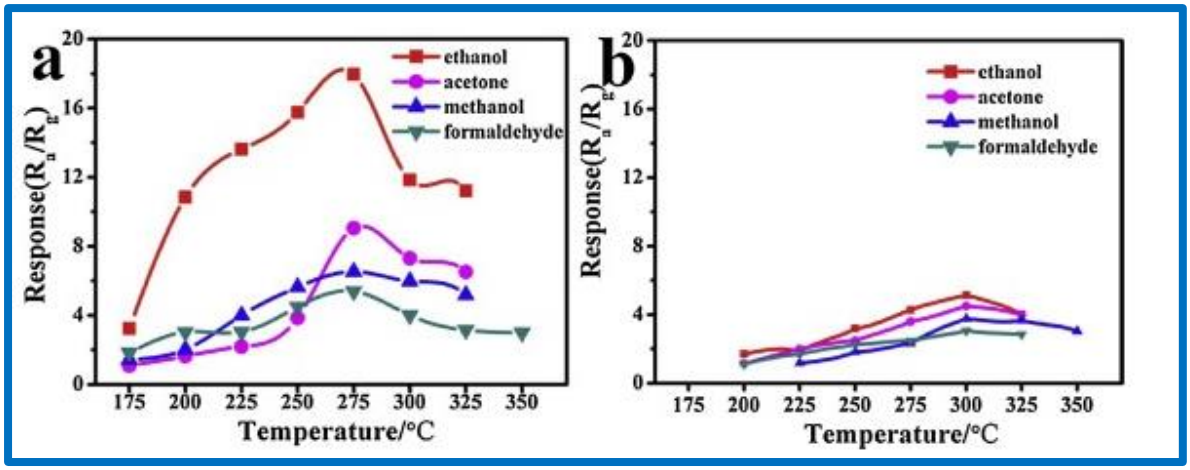

Figure 2 Response of the sample for a particular temperature for composite and for pure ZnO.

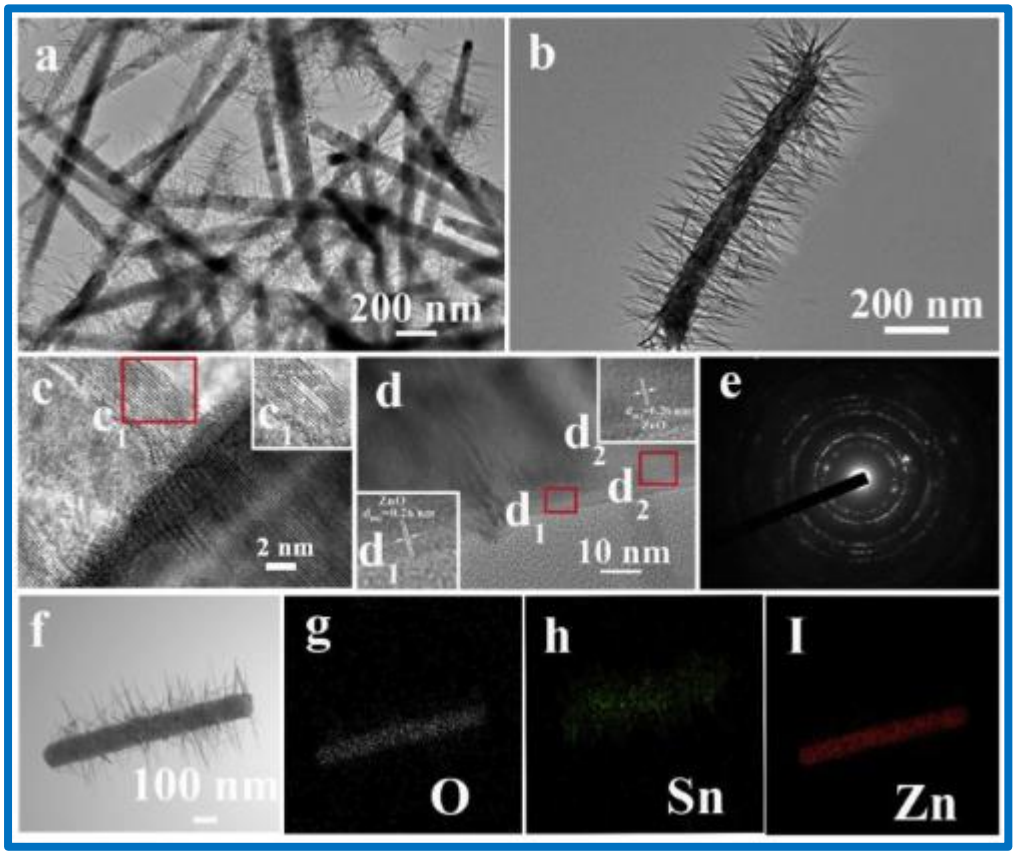

Figure 3 TEM and HR-TEM images of the SnO_2/ZnO sample.

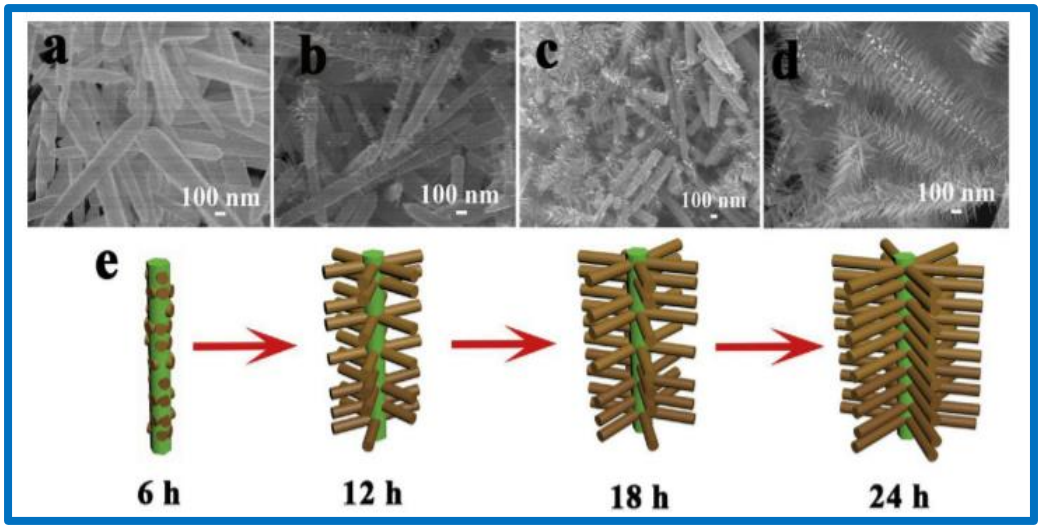

Figure 4 SEM images of (a and b) pure ZnO and (c–f) SnO_2/ZnOheterostructure

2.2 Paper 2

Room temperature highly toxic NO_2 gas sensors based on rootstock/scion nanowires of SnO_2/ZnO, ZnO/SnO_2, SnO_2/SnO_2 and, ZnO/ZnO"(2021).

In this paper composites of SnO_2 and ZnO rootstock/scion nanowires were grown using CVD method.Andgas sensing parameters were studied for NO_2 gas for all the nanostructures.

In studies s found that the SnO_2/ZnO has best sensing properties as compared to all other structures. The study was taken place at 100 ppb for NO_2.

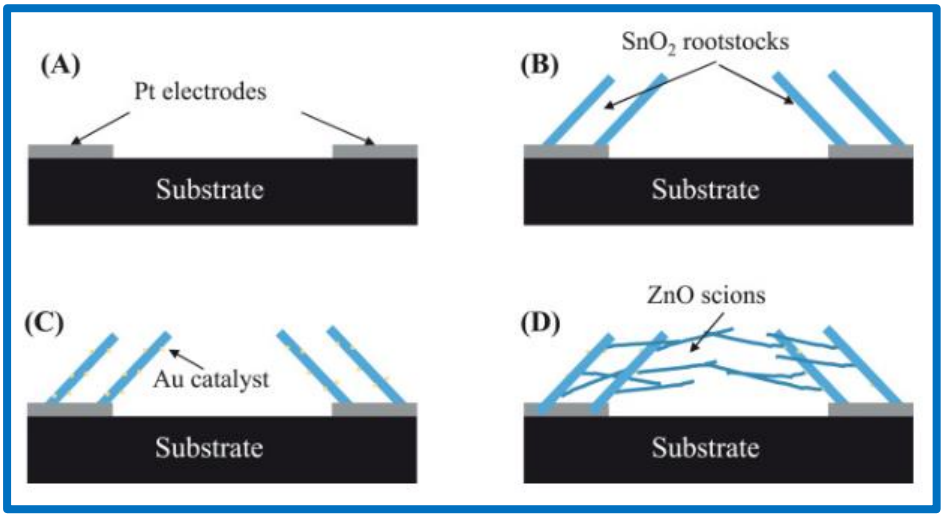

Figure 5 Fabrication process for the grafted nanowires of SnO_2/ZnO NWS.

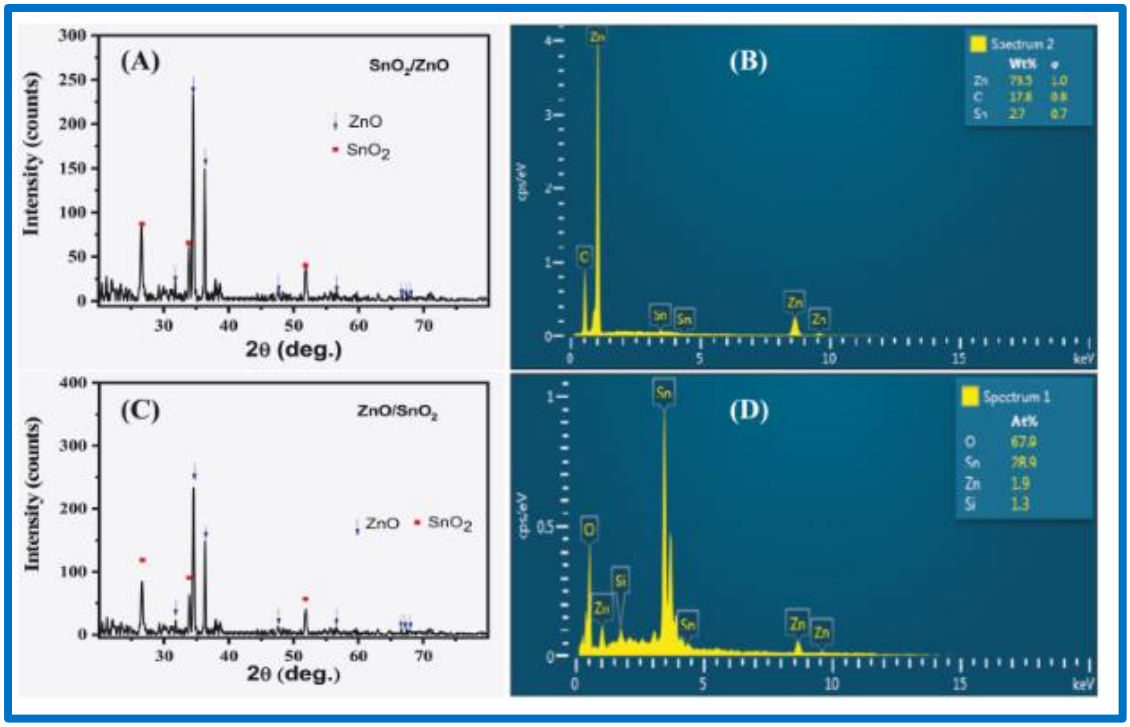

Figure 6 XRD pattern and EDS analysis of the composite samples.

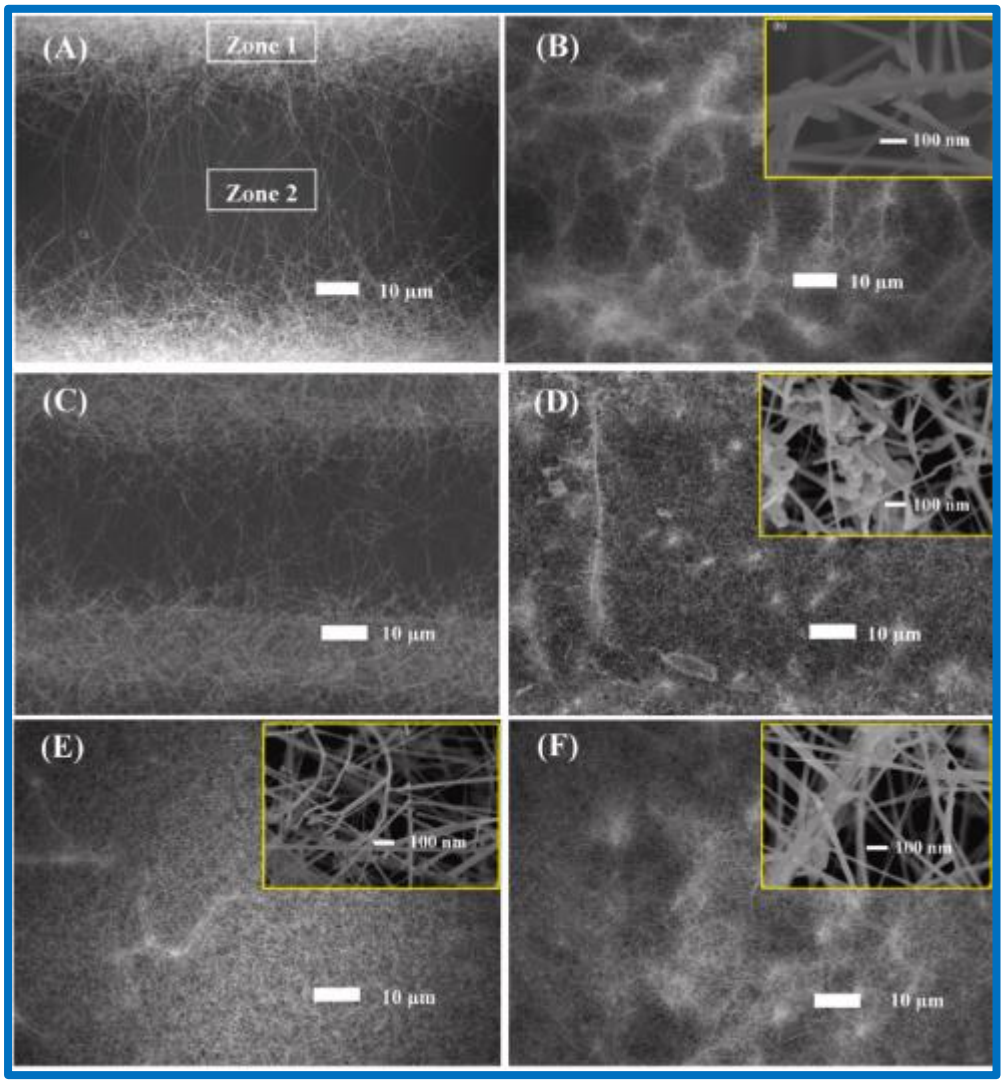

Figure 7 FESEM images for composites.

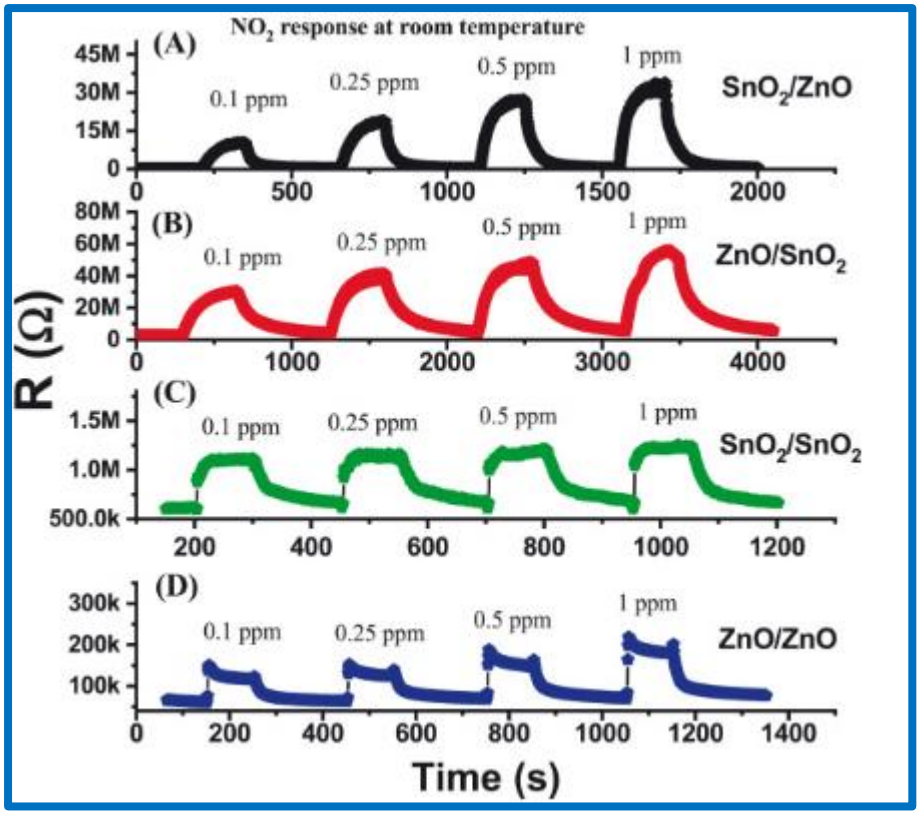

Figure 8 Gas sensing response parameter for different gases.

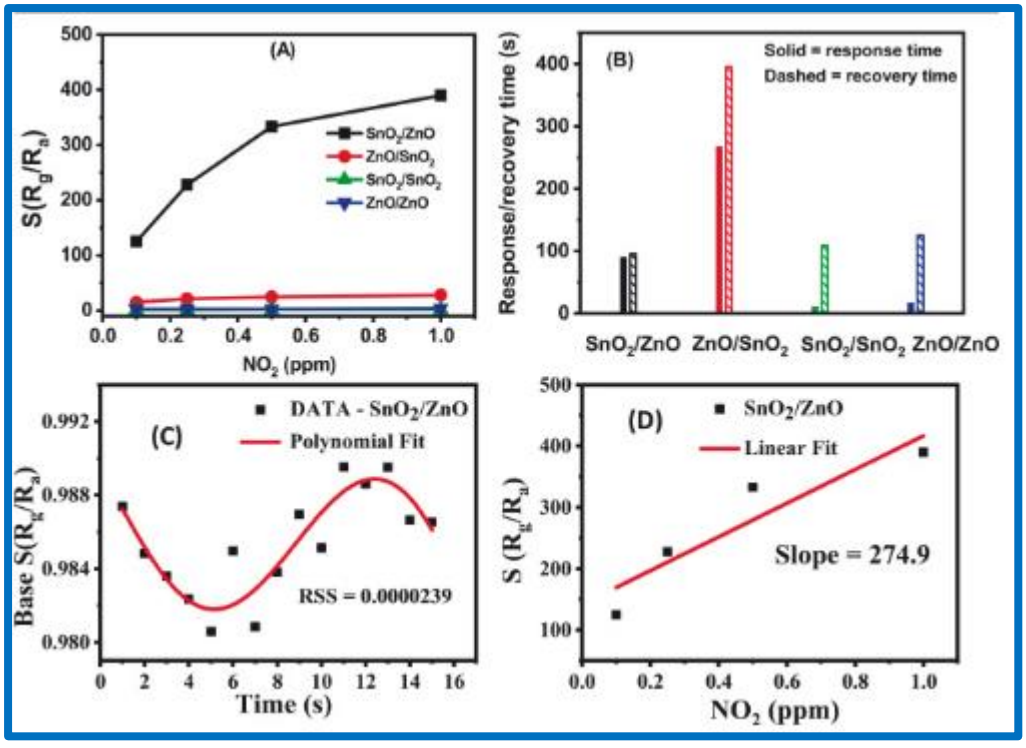

Figure 9 Comparision of gas sensing parameters for all 4 samples.

Result

Composite NWs were grafted using using two step synthesis process.In first step rootstocks were prepared and after that thermal evaporation technique was used to synthesis hetrostructures.TEM and SEM studies showed scions were sucessfully grown on the rootstocks.Gas sensing parameters were studied and it was observed that in concentration between 1 ppm to 100 ppm of NO_2 gas SnO_2 as rootstocks, homo or heterostructures both have similar enhanced properties than that of other two heterostructures(ZnO rootstocks) at 473 K temperature.And SnO_2/ZnO have best gas sensing parameters as comaperd to other three nanocomposites.And this composite is highly selective for the NO_2 gas.

CHAPTER 3

In this chapter complete process of synthesis of SnO_2 and ZnO is discussed with the proper quantity of precursors and other parameters that we have used and characterization of the produced sample using the XRD technique is also discussed.

3. Experimental

To synthesize the various nanostructures, a hydrothermal method was used and the schematic of the typical synthesis route is represented in Fig. 1. In the experimental process, analytical grades of chemical reagents were used as received without any modification.

3.1 Hydrothermal Method:

Compared with the "low-temperature" coprecipitation procedures that usually produce poor crystalline nanoparticles, the hydrothermal synthesis could get magnetic nanostructures with a very high crystalline nature due to their high-temperature and high-pressure reaction conditions. In this case, a water mixture of precursors is heated in a sealed stainless steel autoclave above the normal temperature, and consequently, the pressure within the reaction autoclave is dramatically increased above atmospheric pressure. This effect of high temperature and pressure provides a one-step process to produce highly crystalline materials and we don't need to do post annealing treatments. The reaction parameters, such as the type and concentration of the precursors, the solvent, the stabilizing agents, and the reaction temperature and time, present important effects on the products.

Hydrothermal synthesis refers to the heterogeneous reactions for synthesizing inorganic materials in water above room temperature and pressure. Hydrothermal strategies have been developed to synthesize a large range of nanostructures, including magnetic nanostructures.

Figure 10 Schamatic diagram of Autoclave

3.2Synthesis of SnO_2 nanorods

Firstly, a solution in ethanol-water mixture, containing Tin tetrachloride ($SnCl_4.5H_2O$) (2 mM) and KOH (of 20 mM) was prepared. The solution was then stirred constantly for 50 minutes. The so formed solution was then kept in an oven for 24hrs at 180 °C, after transferring it to a hydrothermal container (Teflon lined stainless steel autoclave). After cooldown at a room temperature, the solution was then centrifuged for 10 minutes at 5000rpm. The white precipitate is collected and washed (three times, using DI) and followed by drying in an oven at 60°C for 24hrs.

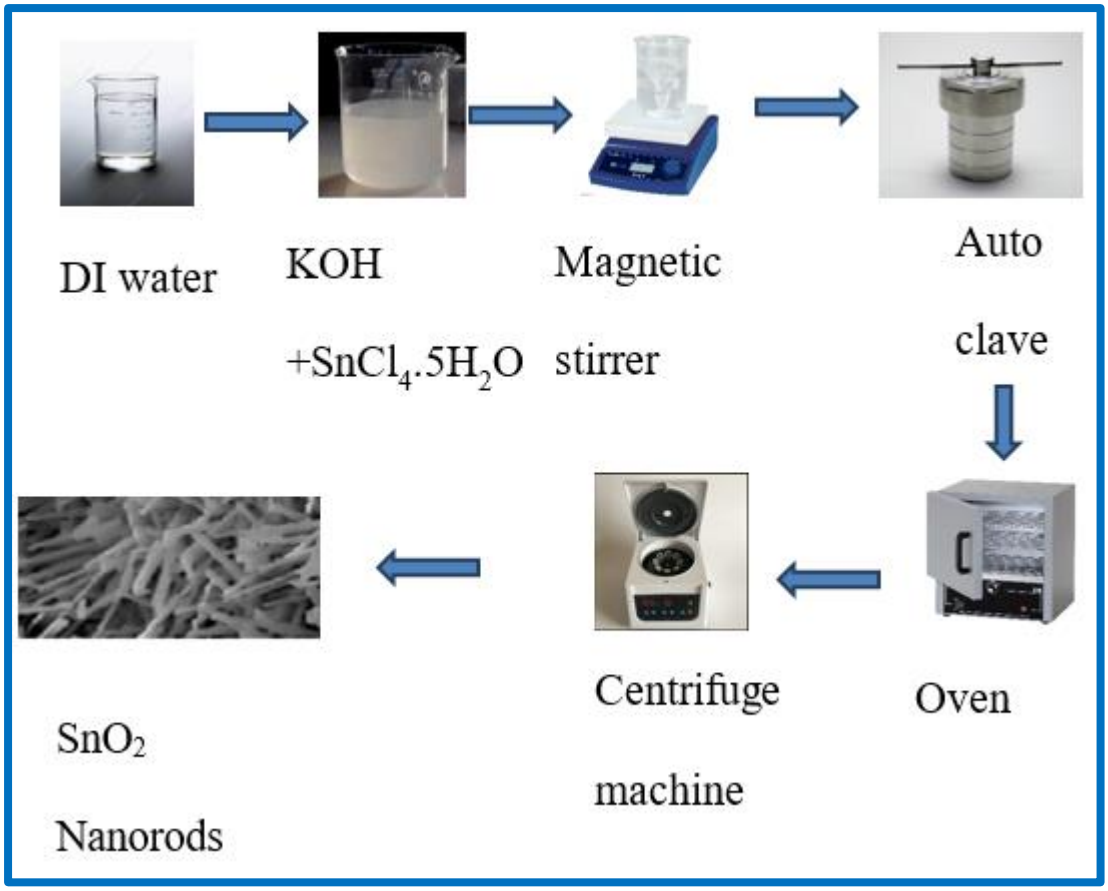

Figure 11 Hydrothermal method for SnO2 nanorods Synthesis.

3.3 Synthesis of ZnO nanorods

An Exactly similar route (as in SnO_2 synthesis) was then used for the synthesis of ZnO nanorods except the concentration of salts and autoclave temperatures. Zinc chloride ($ZnCl_2$) 0.267 g (0.032 M), and sodium carbonate (Na_2CO_3) 26.67 g (4.193 M) were used to prepare the solution in ethanol-water mixture (1/1, V/V). The solution was heated at 140 ^{0}C in the Teflon autoclave for 24 hours [9].

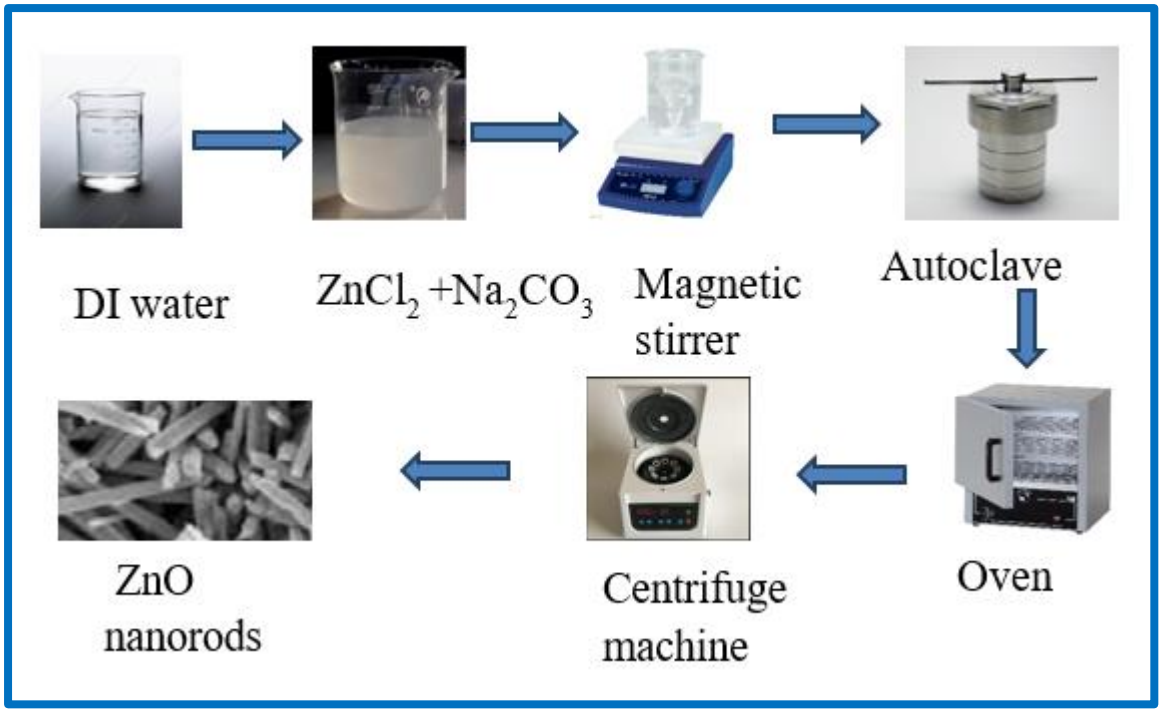

Figure 12 Synthesis of ZnO nanorods by Hydrothermal Method.

3.4 Synthesis of SnO_2/ZnO

2 mmol (2.104 g) of zinc sulfate heptahydrate ($ZnSO_4 \cdot 7H_2O$) and of 1mmol (0.594 g) of tin tetrachloride pentahydrate ($SnCl_4 \cdot {}_5H2O$) were dissolved in an appropriate amount of DI water and then allowed to constantly stir for 20 min. Then to the solution formed above, an addition of 15 mmol of NaOH and then allowed to stir for 20 more minutes. The stirred solution was then kept in an oven for 24hrs at 180 °C, after successfully transferring it to a hydrothermal container (Teflon lined stainless steel autoclave). The after-processing (washing and drying) is carried out the same as was done for the synthesis of ZnO and SnO_2.

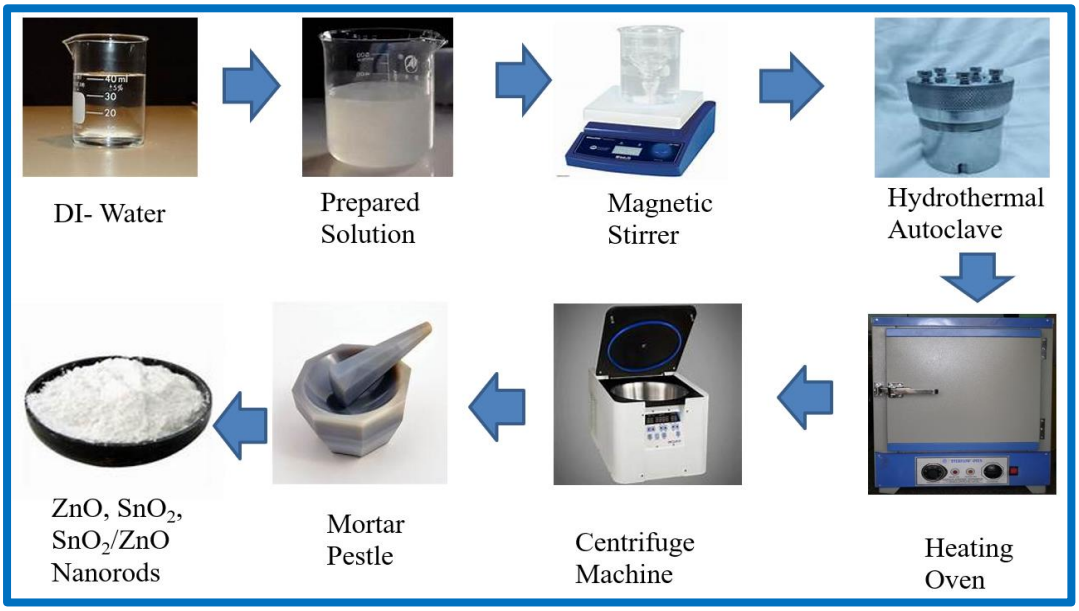

Figure 13 Schematic representation of synthesis process used for pure SnO_2, ZnO and SnO_2/ZnO composite.

CHAPTER 4

4. Results and Discussion

4.1 X-Ray Diffraction:

In the electromagnetic spectrum, the wavelength range of X-rays lies between 0.01 to 10 nm. X – rays were discovered by Wilhelm Conrad Rontgen in 1895. After their discovery, they are continuously being used in the science and technology domains.. And X-ray Diffraction from crystals was discovered by Laue in 1912. Since then, X – Rays are used by material scientists and crystallographers for the characterization of materials**.**

4.2 Bragg's Law:

Based on the phenomena of diffraction through a crystal, Bragg gave a simple formula using interplanar spacing 'd' of crystal planes and 'θ' is the angle of the incidence of X – rays demonstrated in figure13. The formula is written as:

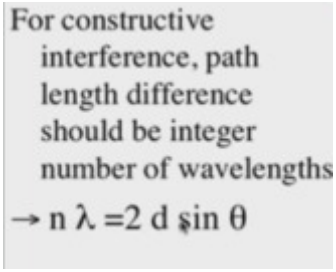

Where λ - wavelength of X – rays

n= 1, 2, 3….

Bragg's law is true for all λ≤ 2d.

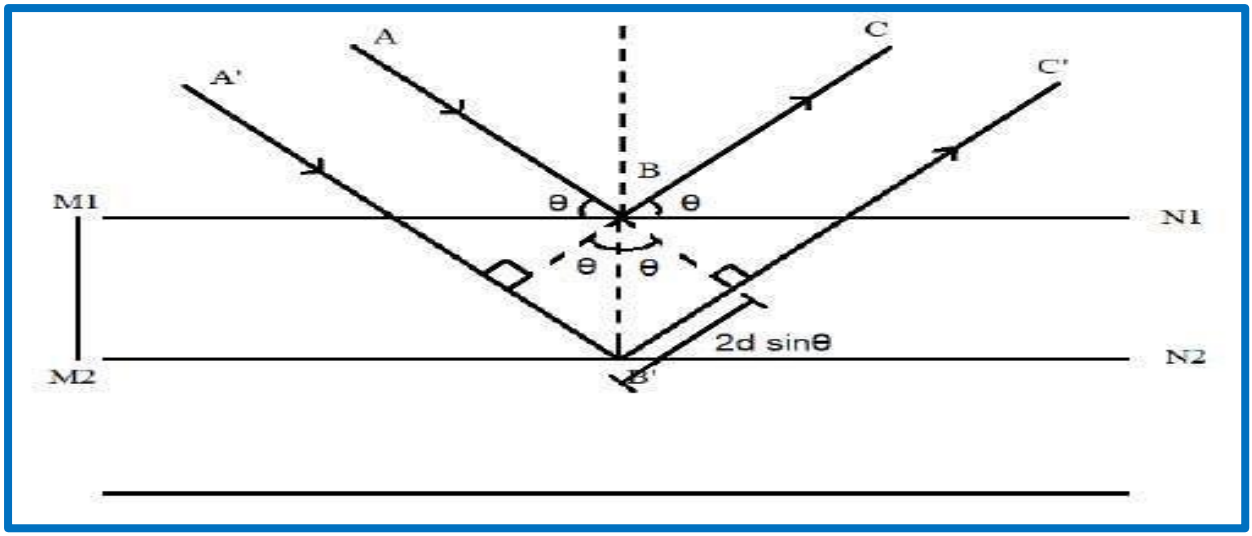

Figure 14 Bragg's Law.

The generated XRD pattern has three information of the sample; space group determined by the location of the peaks, information about the basis is given by the intensity of the peaks, and the determination of crystallite size and strain with the help of width of the peaks.

4.3 X-ray diffraction analysis:

The structural properties of the synthesized nanostructures were analysed using X- ray diffraction (XRD). The obtained XRD pattern of the synthesized samples were shown in Fig. 14. The sharp peaks at different 2θ values in XRD pattern indicates that synthesized nanostructures have good crystallinity and polycrystalline in nature. The 2θ position of all the diffraction peaks of SnO_2 and ZnO are well indexed and found in total agreement with the standard JCPDS [88-0287 and 00-036-0161] data. Which confirms the synthesized nanostructures of SnO_2 and ZnO have tetragonal rutile and hexagonal wurtzite structure, respectively. However, two additional peaks at $2\theta = 55.18^0$, 60.60^0 observed for ZnO nanostructures with very small intensity. These peaks may arise due to the presence of undissolved Na_2CO_3 which was used as a precursor during synthesis. Also, all the major XRD peaks of SnO_2/ZnO composite nanostructures were matched with the peaks of pure SnO_2 and ZnO. It has been observed that composite also has two additional peaks at $2\theta = 55.18^0$, 60.60^0 with very small intensities. The absence of any additional major diffraction peaks suggest that the synthesized SnO_2/ZnO composite has formed a heterojunction of SnO_2 and ZnO without going through any structural deformation and phase transformation.

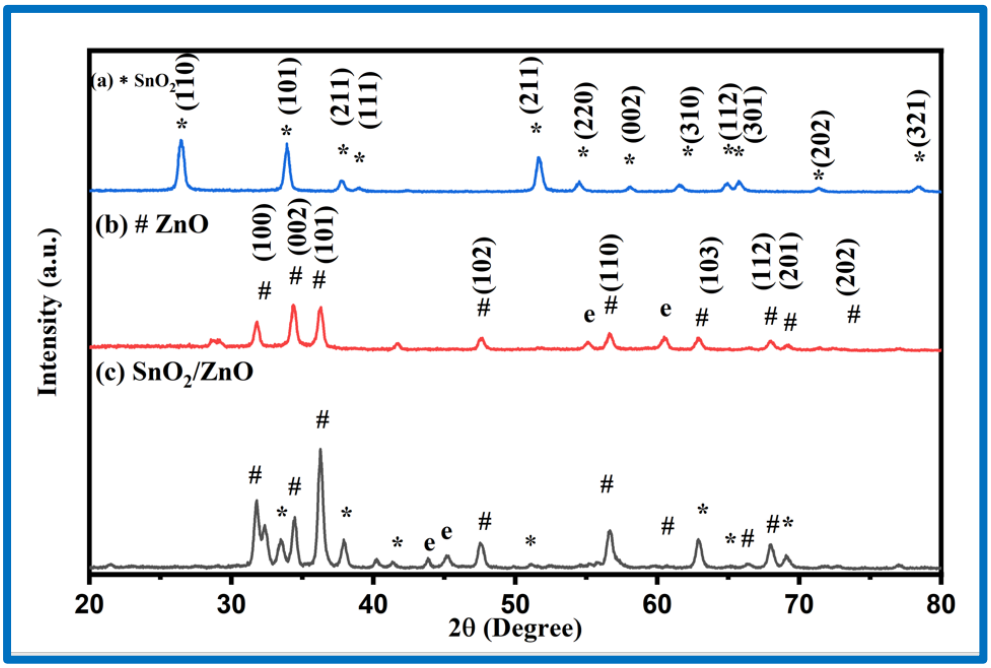

Figure 15 XRD patterns of synthesized (a) SnO_2, (b) ZnO and (c) SnO_2/ZnO composites

Furthermore, the crystallite size was calculated using Scherrer's formula (eq.1) and Williamson-Hall (eq.7) plot and presented in Table 1. It has been observed that crystallite size for all three nanostructures are almost similar. The crystallite size calculated using the W-H method has smaller values as compared to the values calculated using Scherrer formula. It might be because of the Scherrer equation only considers the influence of crystallite size on XRD peak broadening and excludes microstructures of the lattice, such as intrinsic strain, which develops in nanocrystals through point defects, grain boundaries, triple junctions, and stacking faults. However, the variation in crystallite size of the synthesized nanostructures are similarly obtained by both the methods. Also, the other structural parameters of the synthesized nanostructures were calculated using equations 2-4 and tabulated in Table 1. The calculated values of Stacking Fault (SF) and macrostrain (ε) are comparable to the reported data [19]. Smaller values of SF and macrostrain further strengthen that synthesized nanostructures have proper periodic arrangement of lattice planes and almost negligible lattice defects.

(1)

$$D = \frac{K\lambda}{\beta \, cos \, cos \, \theta}$$

(2)

$$\delta = \frac{1}{D^2} \tag{3}$$

$$SF = \left[\frac{[2\pi^2]}{45\sqrt{tan\theta}}\right]\beta \tag{4}$$

$$\varepsilon = \frac{\beta}{4tan\theta}$$

Where λ is wavelength of radiation (1.5406 Å), 'D' is crystallite size, 'k' is constant (0.94), , θ is Bragg's angle in radian and β is the full width at half maximum (FWHM) in radians. In accordance to W-H method the overall broadening (FWHM) of the XRD peaks occurs due to crystallite size (D) and lattice strain (ε) of the nanostructures (eq. 5). Uniform deformation model (UDM) has been considered to obtain the lattice strain and crystallite size. This model assumes the induced lattice strain due to lattice defects and imperfections in the nanomaterials is isotropic in nature [1,2].

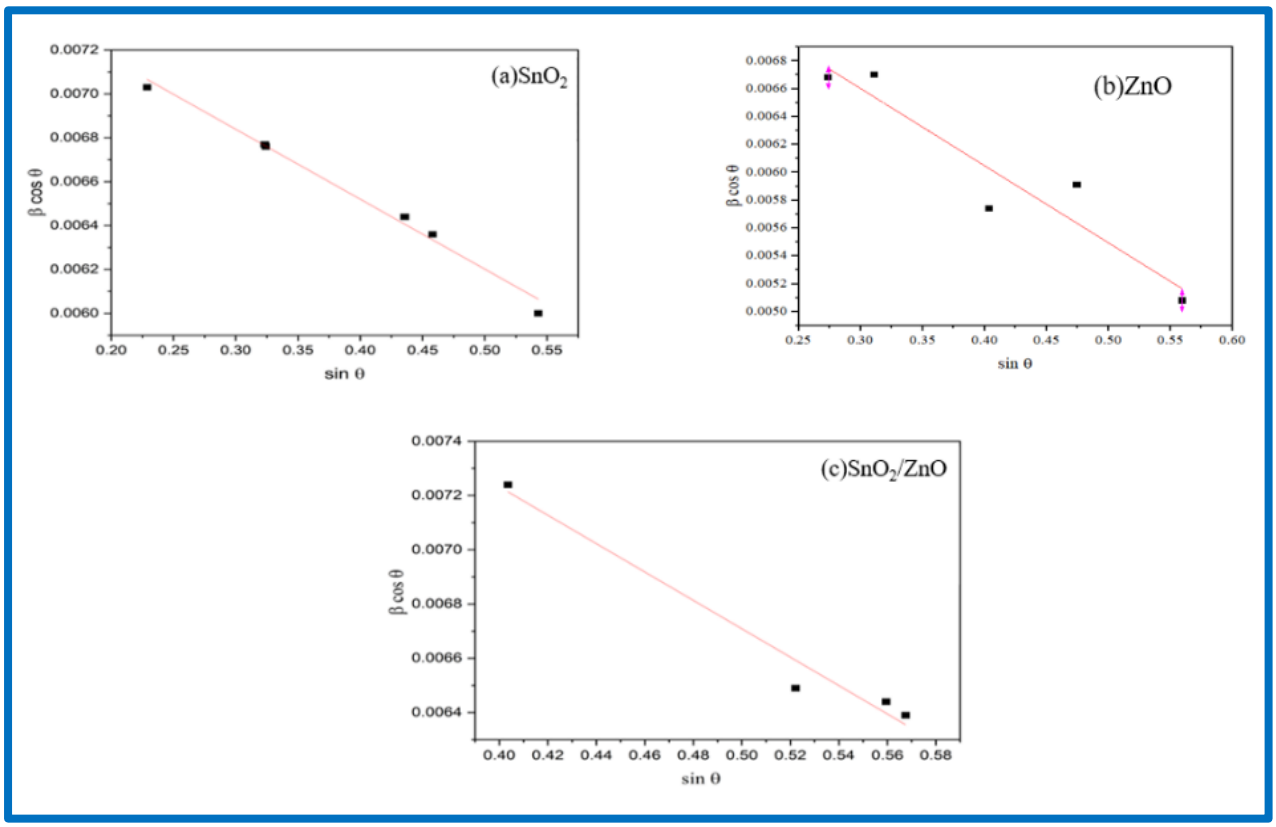

Figure 16 W-H analysis of synthesized (a) Pure SnO_2, (b)Pure ZnO and (c) SnO_2/ZnO composites.

$$\beta_{strain} = 4\varepsilon tan\theta \quad (5)$$

$$\beta_{hkl} = \frac{k\lambda}{D}\frac{1}{cos\theta} + 4\varepsilon tan\theta \quad (6)$$

$$\beta_{hkl}cos\theta = \frac{k\lambda}{D} + 4\varepsilon.sin\theta \quad (7)$$

The y-intercept and slope of the linear fitted line plot of eq. 7 for various crystallographic planes gives the values of crystallite size and lattice strain, respectively. The W-H plot of the synthesized samples are shown in Fig. 15.

Table 1 Calculated values of various structural parameters by using Scherrer equation and W-H Methods from the XRD data.

Sample	Crystallite Size(D) (nm)		Dislocation density(δ)	Stacking Fault (SF)	Micro Strain (ε)	Lattice strain (W-H plot)
	Scherrer's Equation	W-H plot				
Pure SnO_2	32.83	21.40	$9.2x10^{+18}$	0.006309	0.006450	-0.00319
Pure ZnO	35.99	23.85	$7.9x10^{+18}$	0.005423	0.005540	-0.00509
Composite SnO_2/ZnO	34.47	21.63	$9.1x10^{+18}$	0.005517	0.004830	-0.00523

4.4 EDS analysis

The Energy Dispersive X-ray spectroscopy (EDS) analysis of pure SnO_2, pure ZnO and SnO_2/ZnO composite is shown in Figure 16 (a-c). The EDS spectrum confirms the chemical composition of the synthesized nanostructures and absence of any additional major peaks in

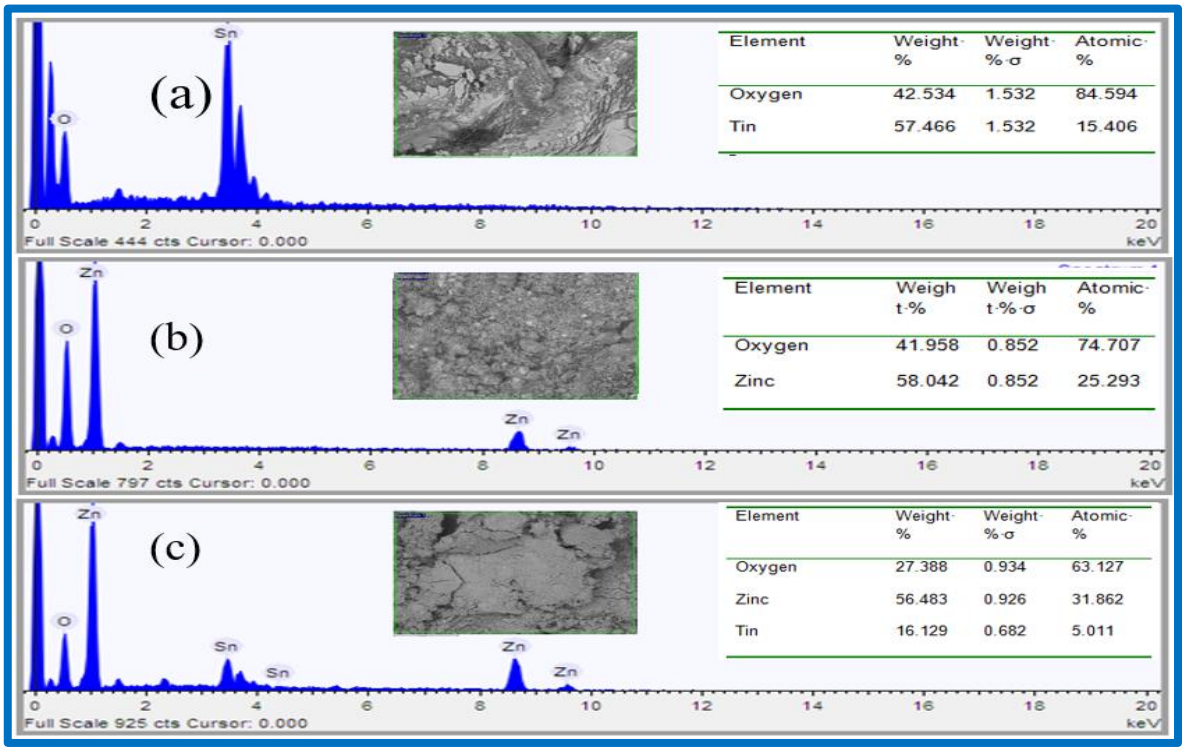

Figure 17 EDS analysis of a) pure SnO_2 nanorods b) pure ZnO nanowires C) SnO_2/ZnO.

spectra suggest that synthesized nanostructures have no impurity [18] [19].

4.5 UV-Visible spectroscopy:

UV-Vis spectroscopy is an expository strategy that measures the sum of discrete wavelengths of UV or unmistakable light that are ingested by or transmitted through a test in comparison to a reference or clear test. This property is affected by the test composition, possibly giving data on what is within the test and at what concentration. Since this spectroscopy method depends on the utilization of light.

How does a UV-Vis spectrophotometer work?

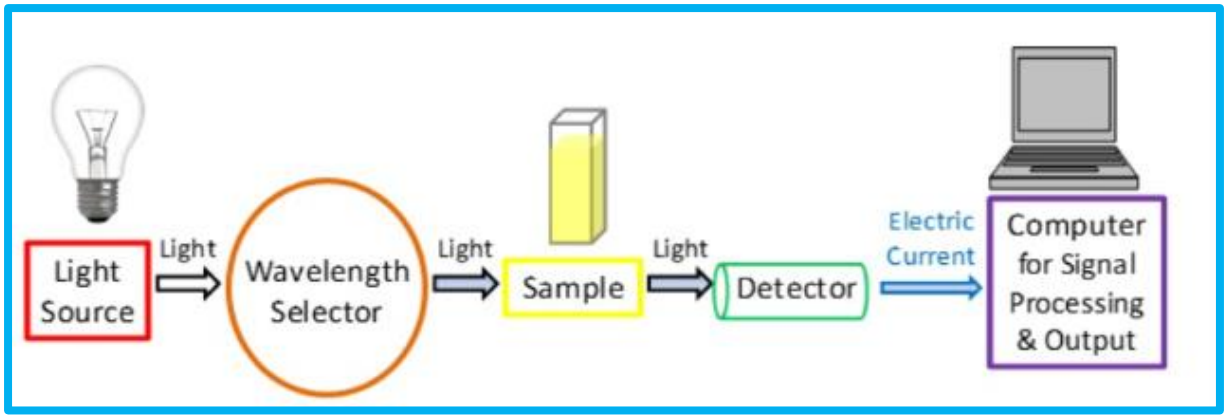

Figure 18 UV-Visible spectroscopy.

The strategy is non-destructive, permitting the test to be reused or continue to advance handling or analyses. Measurements can be made rapidly, permitting simple integration into test protocols. Instruments are simple to utilize, requiring small client preparing earlier to use. Data examination by and large requires negligible preparing, once more meaning small client preparing is required. The instrument is for the most part cheap to secure and work, making it open for numerous laboratories.

The absorbance spectra of pure SnO_2, ZnO, and SnO_2/ZnO composites nanostructure was recorded in the range of 200–800 nm using UV–Visible spectrophotometer at 300 K temperature and shown in Figure 5 (a-c). UV–Visible spectrum shows the information about the excitonic and inter transition of nanostructures. The absorption coefficient (α) has been calculated using Beer-Lambert's law by equation 8.

$$\alpha(\lambda) = \frac{ln\ ln\left(\frac{I}{Io}\right)}{x} = \frac{lnT}{x} = \frac{2.303A}{x} \tag{8}$$

Where I and I_0 are instantaneous and initial value photon intensity, respectively. The thickness of the cuvette is represented by x and A represents the absorbance, which is a unit less quantity [13] [19]. To obtain the optical band gap of synthesized nanostructures we have plotted the Tauc plot between $(\alpha hv)^2$ versus photon energy (hv) as shown in Figure 5 (a-c) by using equation 9.

$$(\alpha hv)^2 = A(hv - E_g)^n \tag{9}$$

where A is a constant (energy independent), α is the absorption coefficient. Eg represents optical band gap while n is another constant which depends on the type of transition.

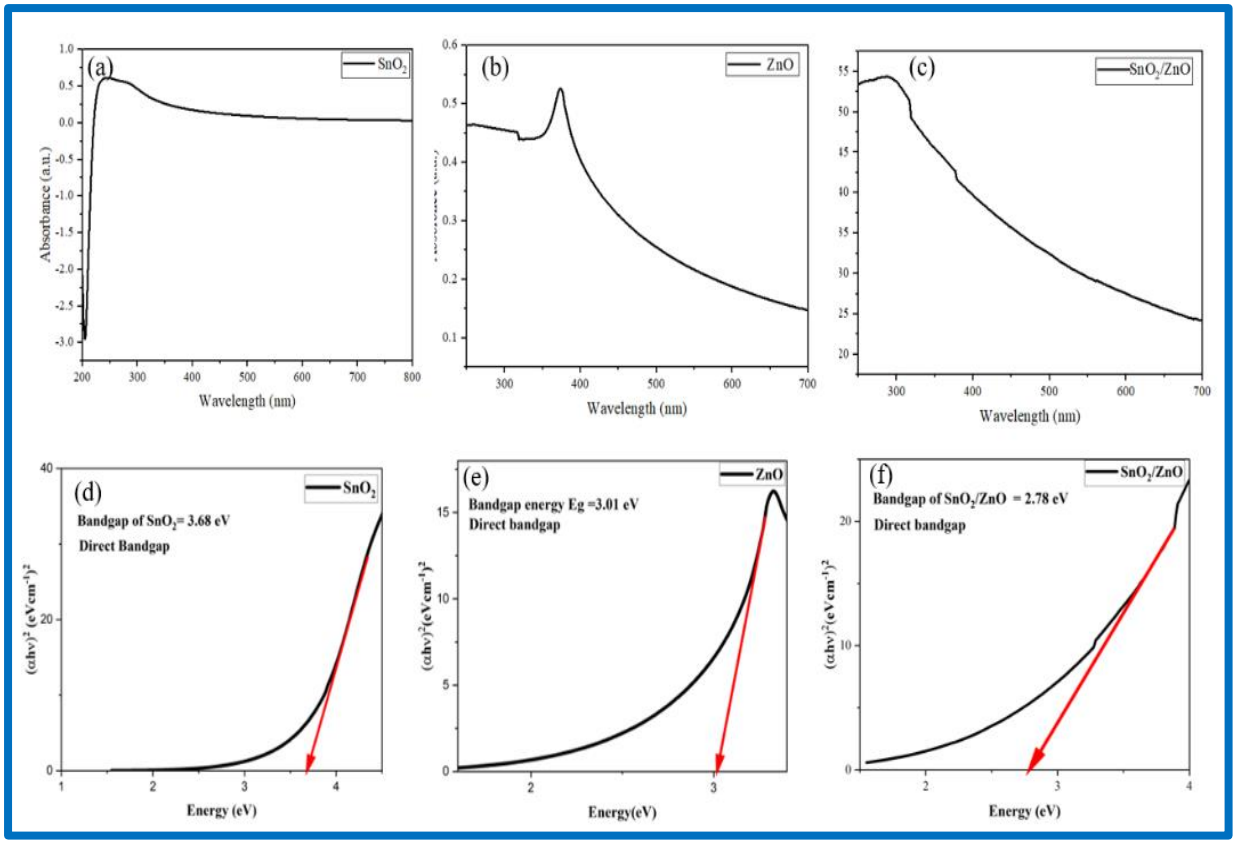

Figure 19 UV-Visible absorption spectrum of pure SnO2, ZnO and SnO2/ZnO and their Tauc plot.

To calculate band gap from the Tauc plot an intercept on x axis (energy axis) obtained by extrapolating the linear portion of the Tauc plot. The obtained values for direct band gap of pure SnO_2, ZnO and SnO_2/ZnO composite are 3.68 eV, 3.01 eV and 2.78 eV respectively. The obtained bandgap results are in accordance with the reported literature [12]. SnO_2/ZnO composite have lower direct band gap than pure ZnO and SnO_2. The reduction in bandgap of composite might be because of the generation of new energy levels of ZnO and SnO_2 on formation of composite nanostructure [12].

4.6 FTIR Analysis

Fourier change infrared (FTIR) spectroscopy tests the vibrational properties of amino acids and cofactors, which are delicate to miniature auxiliary changes. The need of specificity of this strategy, on the one hand, licenses us to test specifically the vibrational properties of nearly all the cofactors, amino corrosive side chains, and of water particles. On the other hand, we will

utilize reaction-induced FTIR distinction spectroscopy to choose vibrations comparing to single chemical bunches included in a particular response. Different strategies are utilized to distinguish the IR marks of each buildup of intrigued within the coming about reaction-induced FTIR distinction spectra.

(Particular) Isotope labeling, site-directed mutagenesis, hydrogen/deuterium trade are regularly utilized to distinguish the chemical bunches. Thinks about on show compounds and the expanding utilize of hypothetical chemistry for typical modes calculations permit us to decipher the IR frequencies in terms of particular auxiliary characteristics of the chemical bunch or atom of intrigued. This audit presents essentials of FTIR spectroscopy strategy and gives particular critical auxiliary and utilitarian data gotten from the examination of the information from the photosystems, utilizing this method.

The FTIR spectra of using ATR (Attenuated total reflection) mode, for ZnO, SnO_2, SnO_2/ZnO composites, the FTIR was recorded and various functional groups were obtained which can be confirmed using different absorption peaks as shown in the plots in Fig. 19. Absorbance band around at 607.6 cm^{-1} could be for O-Sn-O, Sn-O lattice which is in accordance with the results obtained by [23]. Further, the absorptions at 3433 cm^{-1} of infrared spectra assigned to hydroxyl groups of water molecules adsorbed on the outer surface of SnO_2 nanorods. Similarly, the absorption peak appearing at 3478 cm^{-1} in the IR spectrum of ZnO nanorods could be assigned to the O-H vibrations, which confirms the presence of hydroxyl (OH) groups on the external surface of ZnO nanorods. Additionally, the appearance of the absorbance band at 498.5 cm^{-1} confirms the formation of ZnO nanorods as reported in literature [22]. The absorbance band at 3423 cm^{-1} appears in the IR spectrum of SnO_2/ZnO composite [21].

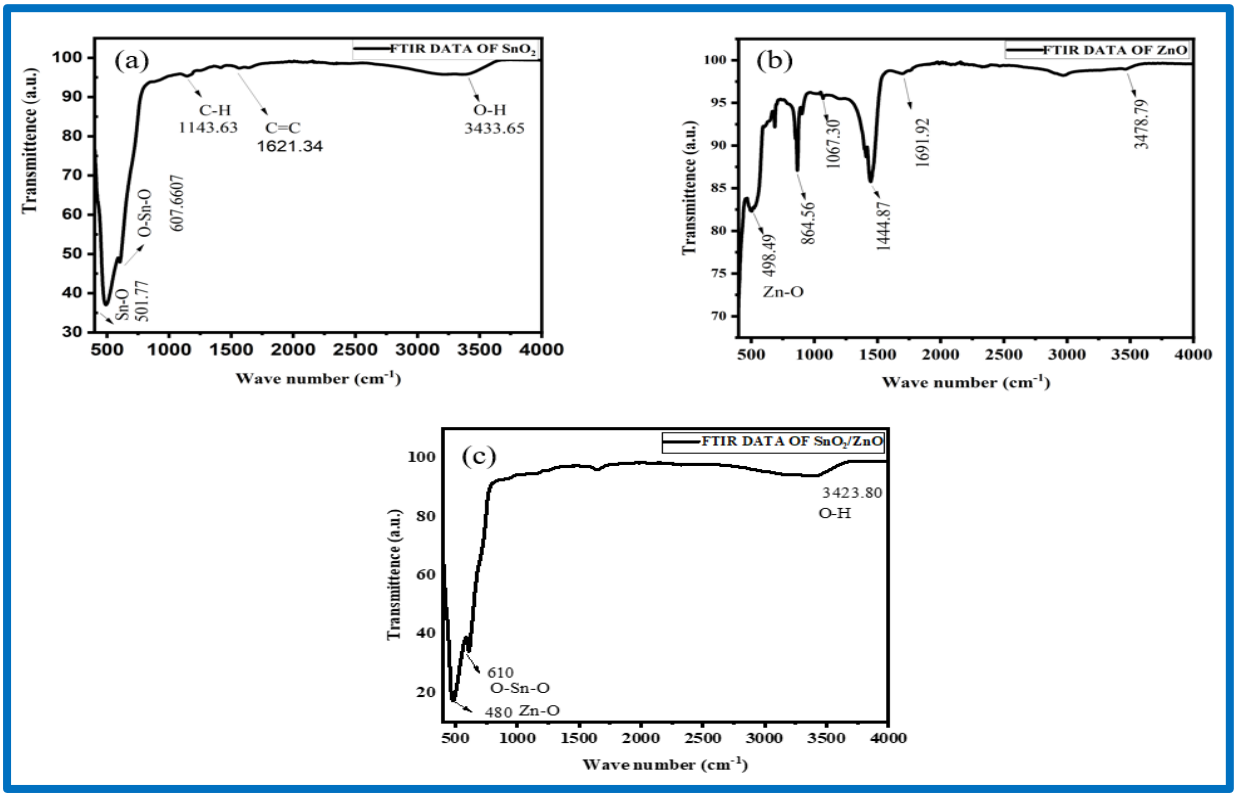

Figure 20 FTIR graphs of pure SnO2, ZnO and SnO2/ZnO composite.

4.7 TEM Analysis

Transmission electron microscopy (TEM) is a method in which a pillar of electrons are transmitted through sample and picture is created by these transmitted electrons.The sample is an ultrathin segmentof size less than 100 nm or suspension on the framwork.Picture is formed from the electrons which are transmitted through the sample.The image is ampified at that point and centered to the imaging gadget, like photographic film, flouroscent screen or scinitillators like sensors joined by charged coupled devices.

TEM magnifying lenses are competent of taking highly resolved images owing to de broglie wavelength of electrons.It helps the instrument to capture small details which are thousands times smaller than a resolvable sample seen in the light magnifying instrument.TEM can be a major stretegy to explain physical,chemical and natural sciences.It can help in investigation of cancer cells, virology and material science.It can be also used to investigate contamination, nanotechnology and semiconductor devices.

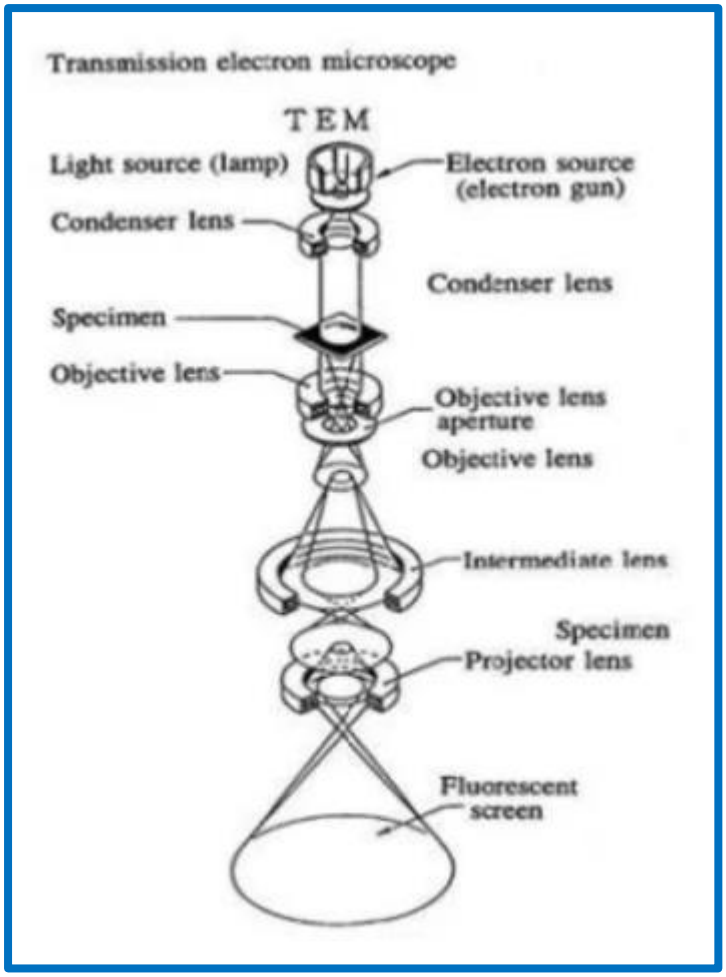

Figure 21 Schamatic diagram of TEM.

The obtained Transmission Electron Microscopic (TEM) images of the synthesized samples are shown in Fig. 21 (a-i) at three different magnifications/scales. It can be observed that the morphology of the synthesized SnO_2, and ZnO are nanobelts and nanorods, respectively. While the nanostructure of SnO_2/ZnO composites is a combination of nanobelts and nanorods as shown in Fig. 21 (g-i). Lattice resolved TEM fringes of surface of the SnO_2, ZnO and SnO_2/ZnO composites are represented in Fig. 22 along with their SAED pattern. The spacing between two neighbouring fringes has been calculated from TEM image (e-f). The obtained average spacing for SnO_2 and ZnO fringes are 0.33 nm and 0.25 nm which correspond to (110) of SnO_2 and ZnO (002) crystal planes. The lattice fringes of SnO_2/ZnO composite with average interplanar spacing of 0.33 mm and 0.25 nm are also matched with (110) and (002) planes of SnO2 and ZnO, respectively. This further confirms that the SnO_2/ZnO composite is a two-phase composite material composed of SnO_2 and ZnO.

The SAED, Figure 8 (a-c), clearly shows the continuous ring diffraction pattern due to the SnO_2 containing a large number of small randomly distributed crystallites for different planes like

(101), (211) and (401). ZnO have SAED pattern showing planes (002) and (103). In composite (002) and (101) planes of SnO_2 and ZnO are overlapping with each other while (110) and (103) planes of ZnO are clearly visible.

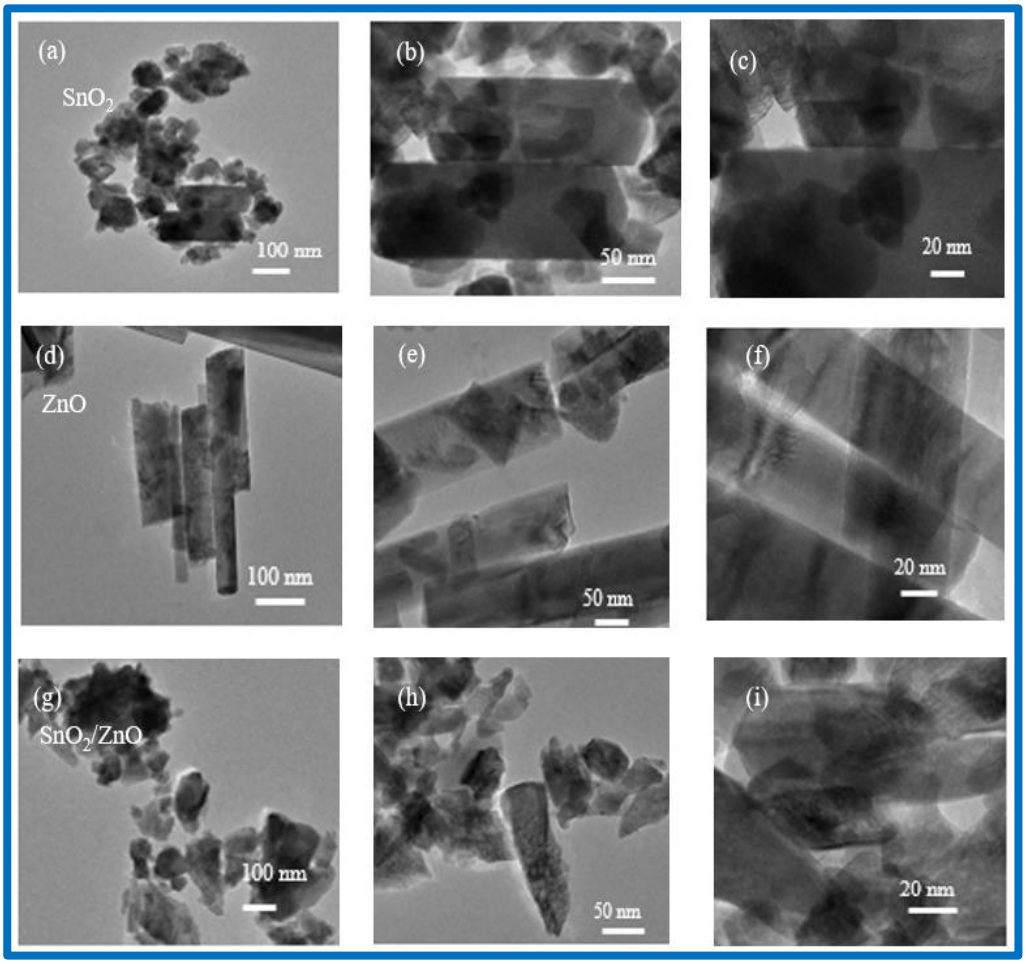

Figure 22 A typical magnification TEM image of (a-c) SnO2 (d-f) ZnO (g-i) SnO2/ZnO.

CHAPTER 5

5. Conclusion and Future scope

Pure SnO_2, ZnO and SnO_2/ZnO composite nanostructures were prepared by using hydrothermal methods. The various structural parameters of synthesized samples were obtained by using Scherrer and W-H Methods. The results indicate that the composites structure has very few additional defects and strain as compared to pure SnO_2 and ZnO. While the observed optical band gap of SnO_2/ZnO composite is smaller than pure SnO_2, and ZnO. Which might be due to generation of new energy levels in the composite structure. The FTIR spectrum further confirms the synthesis of pure SnO_2, pure ZnO and SnO_2/ZnO composites. This study suggests that on synthesis of SnO_2/ZnO composite the structural properties such as phase, lattice strain, defects did not change significantly while the UV-Visible and FTIR absorption peaks get shifted as compared to pure SnO_2 and ZnO. These results are found to be interesting for the application of SnO_2/ZnO composite in the optoelectronic and gas sensing devices.

5.1 Future Scope

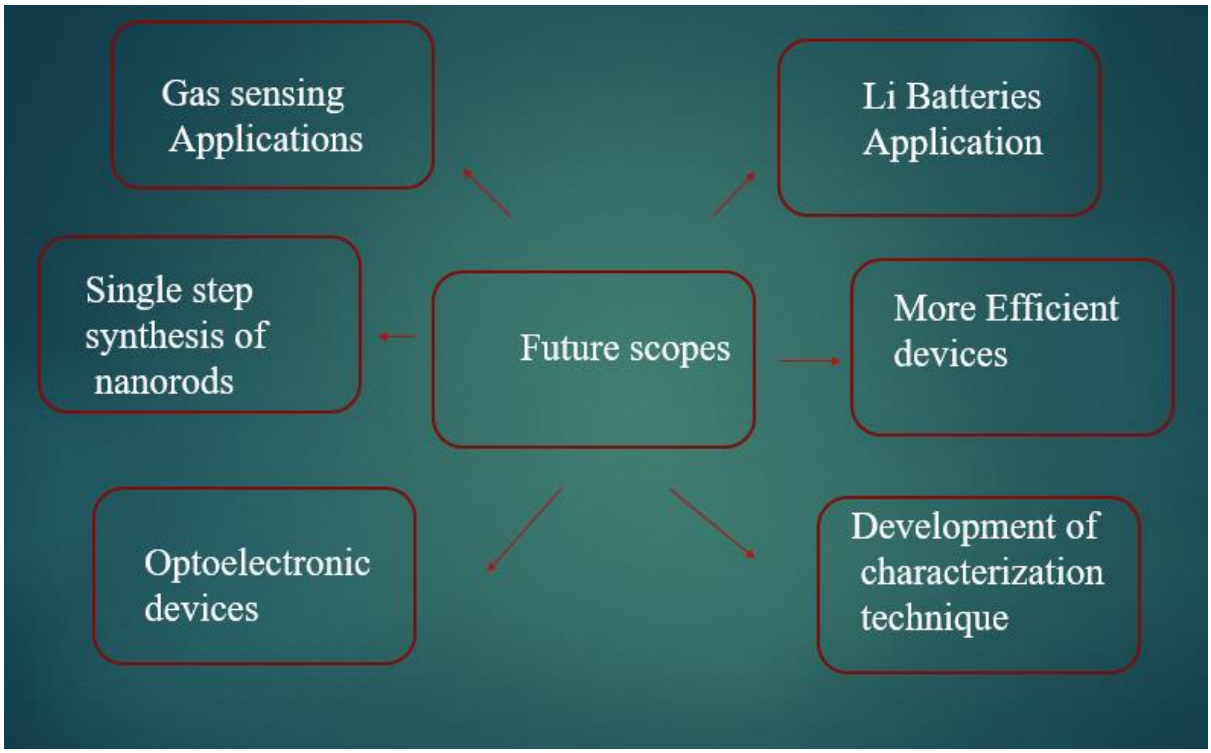

References

1. Guo, J., et al., *High-performance gas sensor based on ZnO nanowires functionalized by Au nanoparticles.* Sensors and Actuators B: Chemical, 2014. 199: p. 339-345.
2. Nowak, R.E., et al., *ZnO Nanorods with Broadband Antireflective Properties for Improved Light Management in Silicon Thin-Film Solar Cells.* Advanced Optical Materials, 2014. 2(1): p. 94-99.
3. Li, H., *Practical evaluation of Li-ion batteries.* Joule, 2019. 3(4): p. 911-914.
4. Khoang, N.D., et al., *Design of SnO2/ZnO hierarchical nanostructures for enhanced ethanol gas-sensing performance.* Sensors and Actuators B: Chemical, 2012. 174: p. 594-601.
5. Zhang, Z., et al., *Novel SnO2@ ZnO hierarchical nanostructures for highly sensitive and selective NO2 gas sensing.* Sensors and Actuators B: Chemical, 2018. 257: p. 714-727.
6. Sun, G., et al., *Core-shell ZnO/SnO2 Nanorods: Two-step Synthesis and Enhanced Ethanol Sensing Performance.* Current Nanoscience, 2015. 11(4): p. 405-412.
7. Kim, J.-H., et al., *Selective H2S sensing without external heat by a synergy effect in self-heated CuO-functionalized SnO2-ZnO core-shell nanowires.* Sensors and Actuators B: Chemical, 2019. 300: p. 126981.
8. Zeng, W., et al., *Hydrothermal synthesis and gas sensing properties of variety low dimensional nanostructures of SnO2.* Physica E: Low-dimensional Systems and Nanostructures, 2013. 47: p. 116-121.
9. Alshehri, N.A., et al., *Investigation of the growth parameters of hydrothermal ZnO nanowires for scale up applications.* Journal of Saudi Chemical Society, 2018. 22(5): p. 538-545.
10. Yang, X., et al., *One step synthesis of branched SnO2/ZnO heterostructures and their enhanced gas-sensing properties.* Sensors and Actuators B: Chemical, 2019. 281: p. 415-423.
11. Alshehri, N.A., et al., *Investigation of the growth parameters of hydrothermal ZnO nanowires for scale up applications.* 2018. 22(5): p. 538-545.
12. Yang, X., et al., *One step synthesis of branched SnO2/ZnO heterostructures and their enhanced gas-sensing properties.* 2019. 281: p. 415-423.

13. Singh, A., S. Sikarwar, and B.C. Yadav, *Design and fabrication of quick responsive and highly sensitive LPG sensor using ZnO/SnO2 heterostructured film.* Materials Research Express, 2021. 8(4): p. 045013.
14. Xu, B., et al., *Structural and optical properties of Zn-doped SnO2 films prepared by DC and RF magnetron co-sputtering.* Superlattices and Microstructures, 2016. 89: p. 34-42.
15. Murali, K. and T. Remadevi, *Rapid Synthesis of SnO2 Thin Films using Monoethanolamine through Wet Chemical Route.* Indian Journal of Science and Technology, 2021. 14(19): p. 1565-1573.
16. Xu, M., et al., *Synthesis, growth mechanism, and photoluminescence property of hierarchical SnO 2 nanoflower-rod arrays: An experimental and first principles study.* 2016. 51(21): p. 9613-9624.
17. Hien, N.T.T., N.X. Dai, and N.N.J.J.-K.P.S. Long, *On the structured green band in ZnO nanowires.* 2008. 52(5): p. 1637.
18. Lu, Z., et al., *Electrospun ZnO–SnO2 composite nanofibers and enhanced sensing properties to SF6 decomposition byproduct H2S.* 2018. 6: p. 540.
19. Meena, D., V.K. Verma, and S. Rana, *Investigation the effect of Zn doping on structural and optical properties of SnO2.* Materials Today: Proceedings, 2021.
20. Bhatia, S., N. Verma, and R. Bedi, *Ethanol gas sensor based upon ZnO nanoparticles prepared by different techniques.* Results in physics, 2017. 7: p. 801-806.

21. Duoc, V. T., Hung, C. M., Nguyen, H., Duy, N. Van, Hieu, N. Van, & Hoa, N. D. (2021). Room temperature highly toxic NO2 gas sensors based on rootstock/scion nanowires of SnO2/ZnO, ZnO/SnO2, SnO2/SnO2 and, ZnO/ZnO. *Sensors and Actuators B: Chemical*, *348*.

22. Yang, X., Zhang, S., yu, Q., Zhao, L., Sun, P., Wang, T., Liu, F., Yan, X., Gao, Y., Liang, X., Zhang, S., & Lu, G. (2019). One step synthesis of branched SnO2/ZnO heterostructures and their enhanced gas-sensing properties. *Sensors and Actuators, B: Chemical*, *281*, . 415–423.

23. Zeng, W., Miao, B., Zhou, Q., & Lin, L. (2013). Hydrothermal synthesis and gas sensing properties of variety low dimensional nanostructures of SnO2. *Physica E: Low-Dimensional Systems and Nanostructures*, *47*.

24 Alshehri, N. A., Lewis, A. R., Pleydell-Pearce, C., & Maffeis, T. G. G. (2018). Investigation of the growth parameters of hydrothermal ZnO nanowires for scale up applications. *Journal of Saudi Chemical Society*, *22*(5)

25. S., Shen, Y., Yan, X., Zhou, P., Yin, Y., Lu, R., Han, C., Cui, B., & Wei, D. (2019). Complex-surfactant-assisted hydrothermal synthesis of one-dimensional ZnO nanorods for high-performance ethanol gas sensor. *Sensors and Actuators, B: Chemical*, *286*, 501–511.

26. Zhao, S., Shen, Y., Maboudian, R., Carraro, C., Han, C., Liu, W., & Wei, D. (2021). Facile synthesis of ZnO-SnO2 hetero-structured nanowires for high-performance NO2 sensing application. *Sensors and Actuators, B: Chemical*, *333*.

27. Zappa, D., Galstyan, V., Kaur, N., Munasinghe Arachchige, H. M. M., Sisman, O., & Comini, E. (2018). "Metal oxide -based heterostructures for gas sensors"- A review. In *Analytica Chimica Acta* (Vol. 1039, pp. 1–23). Elsevier B.V. https://doi.org/10.1016/j.aca.2018.09.020

28. Yang, X., Zhang, S., yu, Q., Zhao, L., Sun, P., Wang, T., Liu, F., Yan, X., Gao, Y., Liang, X., Zhang, S., & Lu, G. (2019). One step synthesis of branched SnO2/ZnO heterostructures and their enhanced gas-sensing properties. *Sensors and Actuators, B: Chemical*, *281*, 415–423.

29. Zhao, B., Dhara, A., Dendooven, J., & Detavernier, C. (2020). Atomic Layer Deposition of SnO2-Based Composite Anodes for Thin-Film Lithium-Ion Batteries. *Frontiers in Energy Research*, *8*. https://doi.org/10.3389/fenrg.2020.609417

30. Huang, Y., Liu, X., Lu, L., Fang, J., Ni, H., & Ji, Z. (2015). Preparation and characterization of ZnO/SnO2 composite thin films as high-capacity anode for lithium-ion batteries. *Applied Physics A: Materials Science and Processing*, *120*(2). https://doi.org/10.1007/s00339-015-9209-x

Materials Today: Proceedings xxx (xxxx) xxx

Contents lists available at ScienceDirect

Materials Today: Proceedings

journal homepage: www.elsevier.com/locate/matpr

Investigation of structural and optical properties of pure SnO_2, ZnO and SnO_2/ZnO composite nanorods

Vineeta Yadav *, Nirmal Singh, Deshraj Meena

Department of Applied Physics, Delhi Technological University, New Delhi 110042, India

ARTICLE INFO

Article history:
Available online xxxx

Keywords:
SnO_2
ZnO
SnO_2/ZnO composite nanorods
Hydrothermal
W-H method

ABSTRACT

Nanorods of SnO_2, ZnO and SnO_2/ZnO composites were successfully synthesised by the hydrothermal method in a one step process under specific conditions. The lattice strain and crystallite size of the nanorods were calculated using Williamson-Hall and Scherrer method. TEM (Transmission Electron Microscopy) results confirm the synthesized samples are nanorods. The various crystalline planes of the nanorods were also identified using SAED (Selected Area Electron Diffraction) Pattern. The EDS (energy dispersive spectroscopy) result confirms the chemical purity of the nanorods. Furthermore, the optical band gap of SnO_2/ZnO nanocomposite was found to be lesser than the pure optical bandgaps of either SnO_2 and ZnO nanorods. Various functional groups were found to be on the surface of the synthesized nanorods, from the FTIR analysis.

Selection and peer-review under responsibility of the scientific committee of the International Conference on Materials, Processing & Characterization.

1. Introduction

In recent years, many applications, including gas sensors [1], solar cells [2], lithium-ion batteries (LIBs), and other opto-electronic nanodevices [5–8] are studied for metal oxide nanowires, nano-tubes and nanofibers (Semi-conductor nanostructures), due to their appreciable electronic structural characteristics, optical properties and various chemical properties. The metal oxides that are formed between metal cations and oxide ions are the chemical compound.Moreover, due to their band gaps being wide and exciton binding energy being high, ZnO, TiO_2, SnO_2, CuO, Fe_2O_3 etc, are earlier reported to be some of best holders of semiconducting properties in metal oxides due to their wide band gap and high exciton binding energy. Tin dioxide (SnO_2) and Zinc oxide (ZnO) have been widely used as photocatalyst for photodegradation of organic compounds, sensing material in resistive gas sensors, perovskite solar cells, liquid crystal display, biosensors, acoustic photodevices and photodiodes, electrochemical supercapacitors, catalysts and in the development of electrode materials for LIBs . Both of these metal oxides have high melting point and large cohesive energy, excellent thermal and mechanical stability, good electrical conductivity, and high transparency in the visible spectrum. These properties make them obvious for the above application. Moreover, both are easily available and environment friendly. It has been observed that to obtain the desired materials with enhanced properties, the nanostructures of SnO_2 and ZnO composite has been used in many applications [3,4]. Due to creation of more electron and efficient transport of charge carriers in the composites of nanostructure have better properties. The efficiency for the devices based on pure metals are lower than the devices based on SnO_2/ZnO nanocomposites as reported in previous literature. Composites are advantageous as they have been found more porous in comparison with the pure metal oxides. Especially, SnO_2 can be made porous with the addition of ZnO in very small amounts [9–11].

In the present work, a comparative analysis of the structural and optical properties of SnO_2/ZnO nanocomposites with pure SnO_2 and ZnO has been done. The nanorods of the pure SnO_2, ZnO and SnO_2/ZnO composites were synthesized using hydrothermal method. The results reveal that the composites have lower optical band gap in comparison with pure SnO_2 and ZnO. The efficiency of charge separation is greatly improved by threshold energy difference of SnO_2 and ZnO, thus improving the optical properties.

Abbreviations: WH-Method, Williamson-Hall Method.

* Corresponding author. Tel.: +91-9140171561.
E-mail address: yadavvineeta38@gmail.com (V. Yadav).

https://doi.org/10.1016/j.matpr.2022.04.255
2214-7853/
Selection and peer-review under responsibility of the scientific committee of the International Conference on Materials, Processing & Characterization.

Please cite this article as: V. Yadav, N. Singh and D. Meena, Investigation of structural and optical properties of pure SnO_2, ZnO and SnO_2/ZnO composite nanorods, Materials Today: Proceedings, https://doi.org/10.1016/j.matpr.2022.04.255

2. Experimental

To synthesize the various nanostructures, a hydrothermal method was used and the schematic of the typical synthesis route is represented in Fig. 1. In the experimental process, analytical grades of chemical reagents were used as received without any modification.

2.1. Synthesis of SnO_2 nanorods

Firstly, A solution in ethanol–water mixture, containing Tin tetrachloride ($SnCl_4{\cdot}5H_2O$) (2 mM) and KOH (of 20 mM) was prepared. The solution was then stirred constantly for 50 min. The so formed solution was then kept in an oven for 24 hrs at 180 °C, after transferring it to a hydrothermal container (Teflon lined stainless steel autoclave). After cooldown at a room temperature, the solution was then centrifuged for 10 min at 5000 rpm. The white precipitate is collected and washed (three times, using DI) and followed by drying in an oven at 60 °C for 24hrs.

2.2. Synthesis of ZnO nanorods

An Exactly similar route (as in SnO_2 synthesis) was then used for the synthesis of ZnO nanorods except the concentration of salts and autoclave temperatures. Zinc chloride ($ZnCl_2$) 0.267 g (0.032 M), and sodium carbonate (Na_2CO_3) 26.67 g (4.193 M) were used to prepare the solution in ethanol–water mixture (1/1, V/V). The solution was heated at 140 ^{0}C in the Teflon autoclave for 24 hrs.

2.3. Synthesis of SnO_2/ZnO

2 mmol (2.104 g) of zinc sulfate heptahydrate ($ZnSO_4{\cdot}7H_2O$) and of 1 mmol (0.594 g) of tin tetrachloride pentahydrate ($SnCl_4{\cdot}5H_2O$) were dissolved in an appropriate amount of DI water and then allowed to constantly stir for 20 min. Then to the solution formed above, an addition of 15 mmol of NaOH and then allowed to stir for 20 more minutes. The stirred solution was then kept in an oven for 24 hrs at 180 °C, after successfully transferring it to a hydrothermal container (Teflon lined stainless steel autoclave). The after-processing (washing and drying) is carried out the same as was done for the synthesis of ZnO and SnO_2.

3. Results and discussion

3.1. X-ray diffraction analysis:

The structural properties of the synthesized nanostructures were analysed using X- ray diffraction (XRD). The obtained XRD pattern of the synthesized samples were shown in Fig. 2. The sharp peaks at different 2θ values in XRD pattern indicates that synthesized nanostructures have good crystallinity and polycrystalline in nature. The 2θ position of all the diffraction peaks of SnO_2 and ZnO are well indexed and found in total agreement with the standard JCPDS [88–0287 and 00–036-0161] data. Which confirms the synthesized nanostructures of SnO_2 and ZnO have tetragonal rutile and hexagonal wurtzite structure, respectively. However, two additional peaks at $2\theta = 55.18^0$, 60.60^0 observed for ZnO nanostructures with very small intensity. These peaks may arise due to the presence of undissolved Na_2CO_3 which was used as a precursor during synthesis. Also, all the major XRD peaks of SnO_2/ZnO composite nanostructures were matched with the peaks of pure SnO_2 and ZnO. It has been observed that composite also has two additional peaks at $2\theta = 55.18^0$, 60.60^0 with very small intensities. The absence of any additional major diffraction peaks suggest that the synthesized SnO_2/ZnO composite has formed a heterojunction of SnO_2 and ZnO without going through any structural deformation and phase transformation.

Furthermore, the crystallite size was calculated using Scherrer's formula (eq.1) and Williamson-Hall (eq.7) plot and presented in Table 1. It has been observed that crystallite size for all three nanostructures are almost similar. The crystallite size calculated

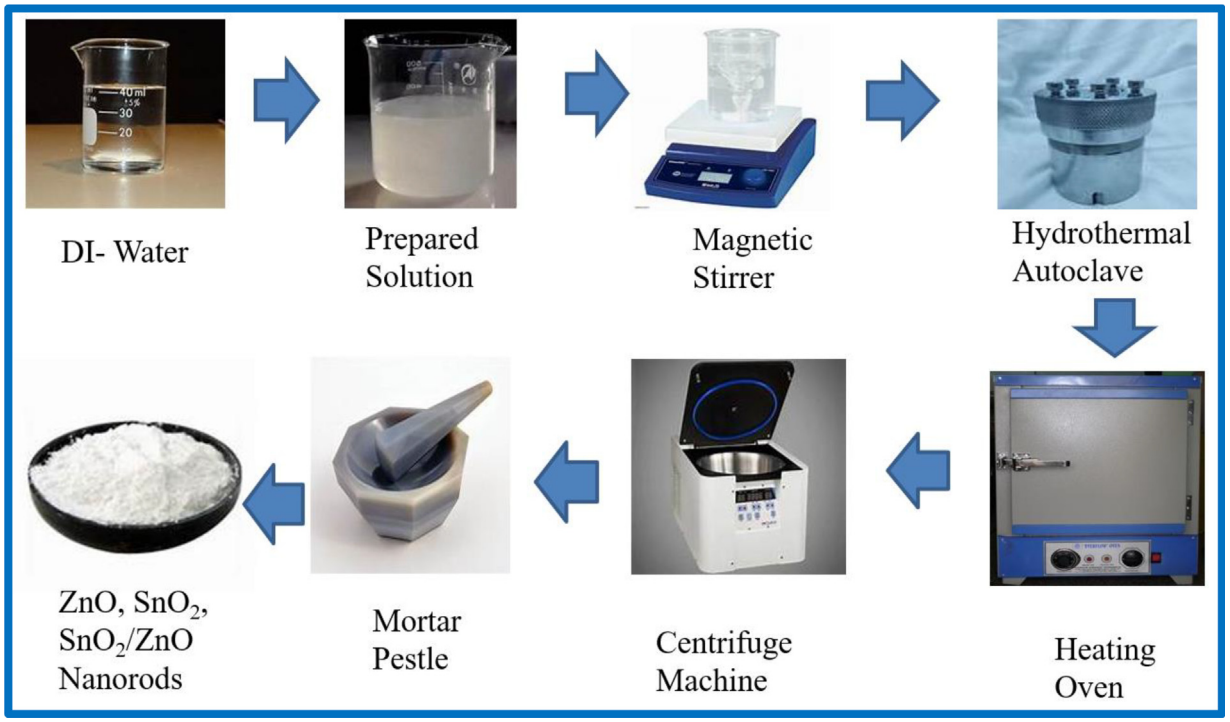

Fig. 1. Schematic representation of synthesis process used for pure SnO_2, ZnO and SnO_2/ZnO composite.

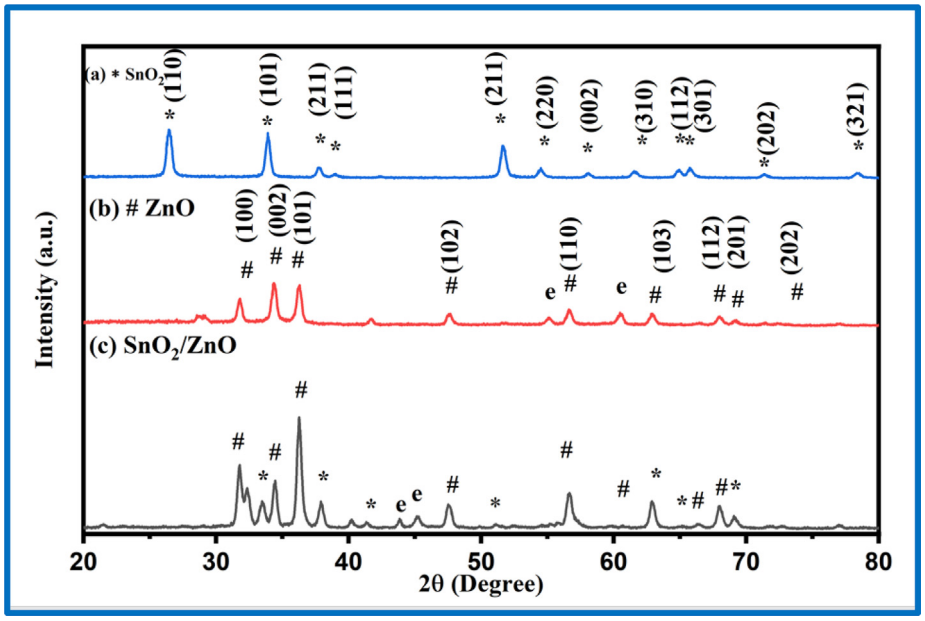

Fig. 2. XRD patterns of synthesized (a) SnO_2, (b) ZnO and (c) SnO_2/ZnO composites.

Table 1
Calculated values of various structural parameters by using Scherrer equation and W-H Methods from the XRD data.

Sample	Crystallite Size(D) (nm)		Dislocation density(δ)	Stacking Fault (SF)	Micro Strain (ε)	Lattice strain (W-H plot)
	Scherrer's Equation	W-H plot				
Pure SnO_2	32.83	21.40	$9.2x10^{+18}$	0.006309	0.006450	−0.00319
Pure ZnO	35.99	23.85	$7.9x10^{+18}$	0.005423	0.005540	−0.00509
CompositeSnO_2/ZnO	34.47	21.63	$9.1x10^{+18}$	0.005517	0.004830	−0.00523

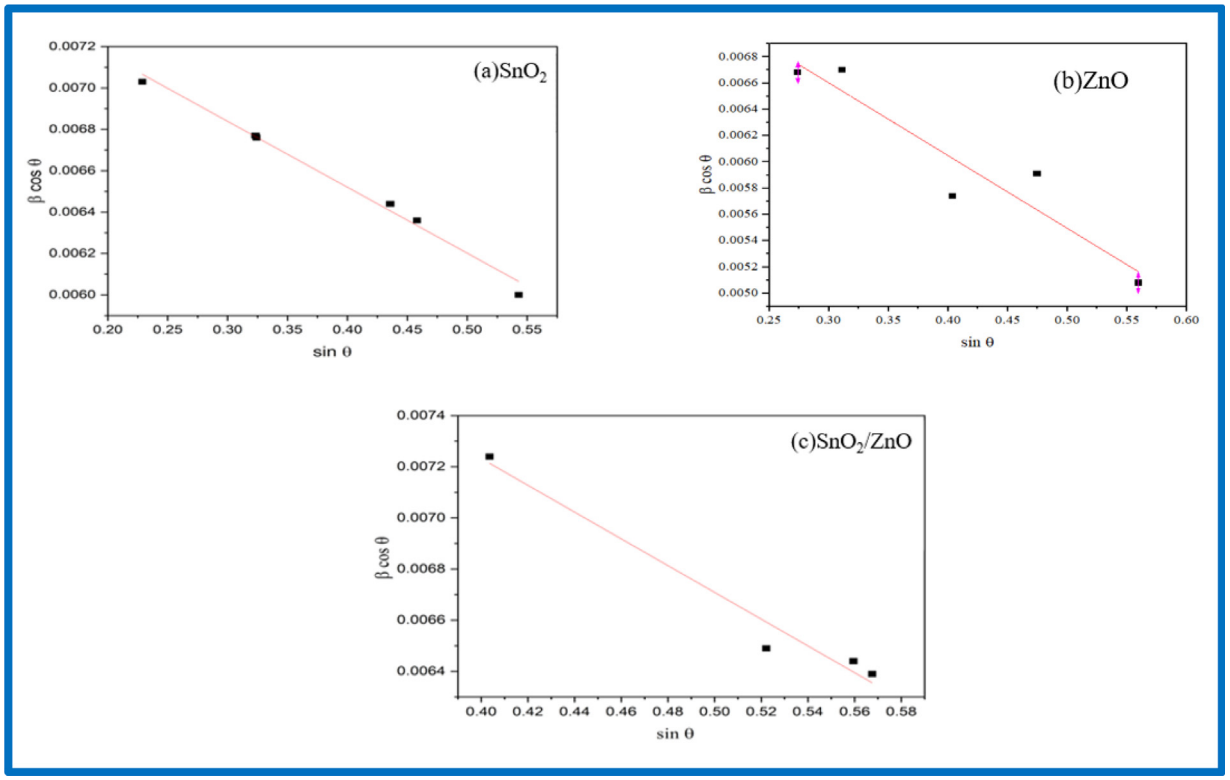

Fig. 3. W-H analysis of synthesized (a) SnO_2, (b) ZnO and (c) SnO_2/ZnO composites.

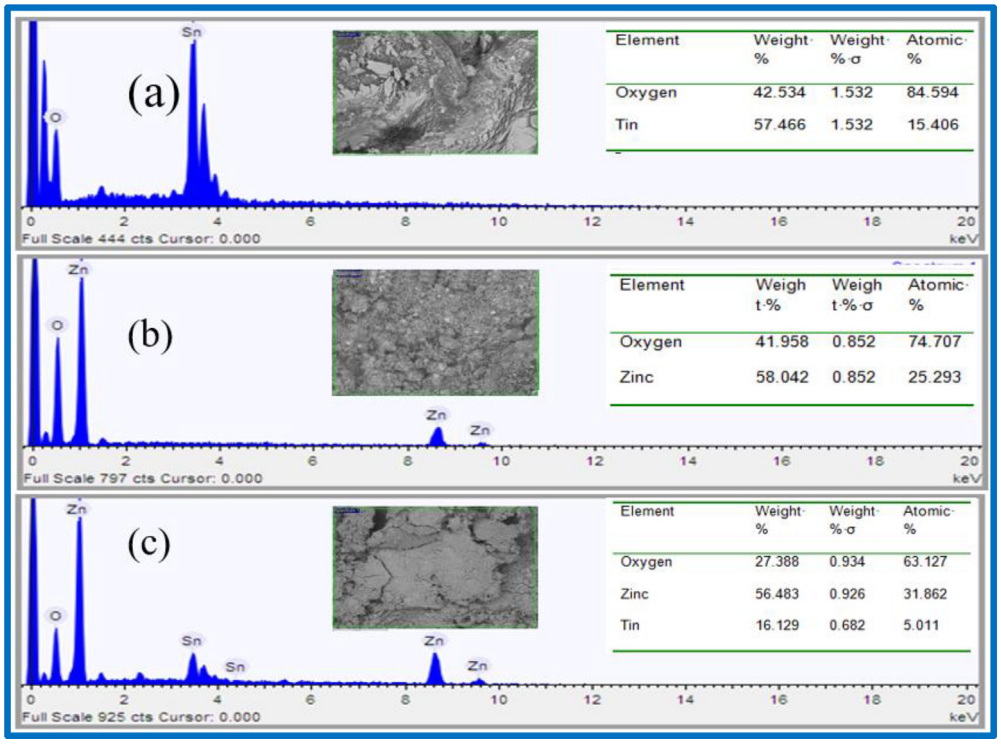

Fig. 4. EDS analysis of a) pure SnO_2 nanorods b) pure ZnO nanowires C) SnO_2/ZnO.

using the W-H method has smaller values as compared to the values calculated using Scherrer formula. It might be because of the Scherrer equation only considers the influence of crystallite size on XRD peak broadening and excludes microstructures of the lattice, such as intrinsic strain, which develops in nanocrystals through point defects, grain boundaries, triple junctions, and stacking faults. However, the variation in crystallite size of the synthesized nanostructures are similarly obtained by both the methods. Also, the other structural parameters of the synthesized nanostructures were calculated using equations 2–4 and tabulated in Table 1. The calculated values of Stacking Fault (SF) and macrostrain (ε) are comparable to the reported data [12]. Smaller values of SF and macrostrain further strengthen that synthesized nanostructures have proper periodic arrangement of lattice planes and almost negligible lattice defects.

$$D = \frac{K\lambda}{\beta coscos\theta} \tag{1}$$

$$\delta = \frac{1}{D^2} \tag{2}$$

$$SF = \left[\frac{[2\pi^2]}{45\sqrt{tan\theta}}\right]\beta \tag{3}$$

$$\varepsilon = \frac{\beta}{4tan\theta} \tag{4}$$

Where λ is wavelength of radiation (1.5406 Å),'k' is constant (0.94),'D' is crystallite size,θ is Bragg's angle and β is the full width at half maximum (FWHM) in radians. In accordance to W-H method the overall broadening (FWHM) of the XRD peaks occurs due to crystallite size (D) and lattice strain (ε) of the nanostructures (eq. (5)). Uniform deformation model (UDM) has been considered to obtain the lattice strain and crystallite size. This model assumes the induced lattice strain due to lattice defects and imperfections in the nanomaterials is isotropic in nature.

$$\beta_{strain} = 4\varepsilon.tan\theta \tag{5}$$

$$\beta_{hkl} = \frac{k\lambda}{D}\frac{1}{cos\theta} + 4\varepsilon tan\theta \tag{6}$$

$$\beta_{hkl}cos\theta = \frac{k\lambda}{D} + 4\varepsilon.sin\theta \tag{7}$$

The y-intercept and slope of the linear fitted line plot of eq. (7) for various crystallographic planes gives the values of crystallite size and lattice strain, respectively. The W-H plot of the synthesized samples are shown in Fig. 3[12].

3.2. EDS analysis

The Energy Dispersive X-ray spectroscopy (EDS) analysis of pure SnO_2, pure ZnO and SnO_2/ZnO composite is shown in Fig. 4 (a-c). The EDS spectrum confirms the chemical composition of the synthesized nanostructures and absence of any additional major peaks in spectra suggest that synthesized nanostructures have no impurity [12].

3.3. the UV–Visible spectroscopy:

2.4. The absorbance spectra of SnO_2, ZnO, and SnO_2/ZnO composites nanostructure was recorded in the range of 200–800 nm using UV–Visible spectrophotometer at 300 K temperature and shown in Fig. 5 (a-c). UV–Visible spectrum shows the information about the excitonic and inter transition of nanostructures. The absorption coefficient (α) has been calculated using Beer-Lambert's law by equation (8).

$$\alpha(\lambda) = \frac{lnln\left(\frac{I}{I_0}\right)}{x} = \frac{lnT}{x} = \frac{2.303A}{x} \tag{8}$$

Where I and I_0 are instantaneous and initial value photon intensity, respectively. The thickness of the cuvette is represented

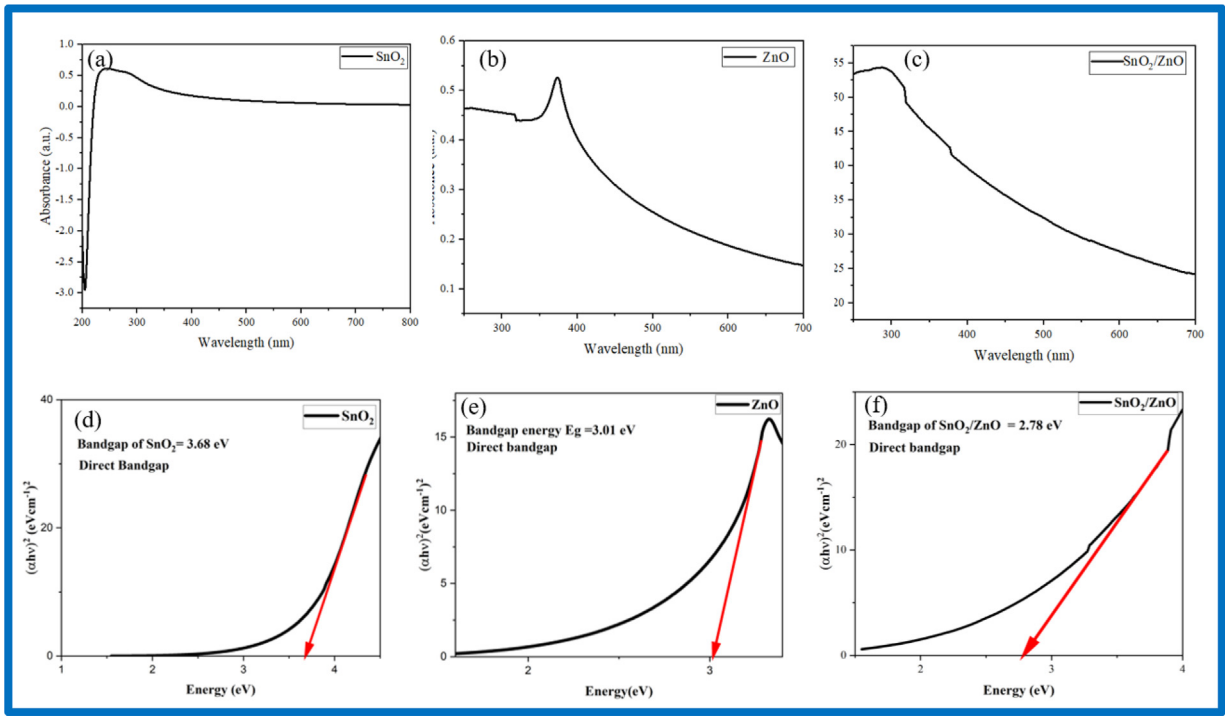

Fig. 5. UV–Visible absorption spectrum of pure SnO_2, ZnO and SnO_2/ZnO and their Tauc plot.

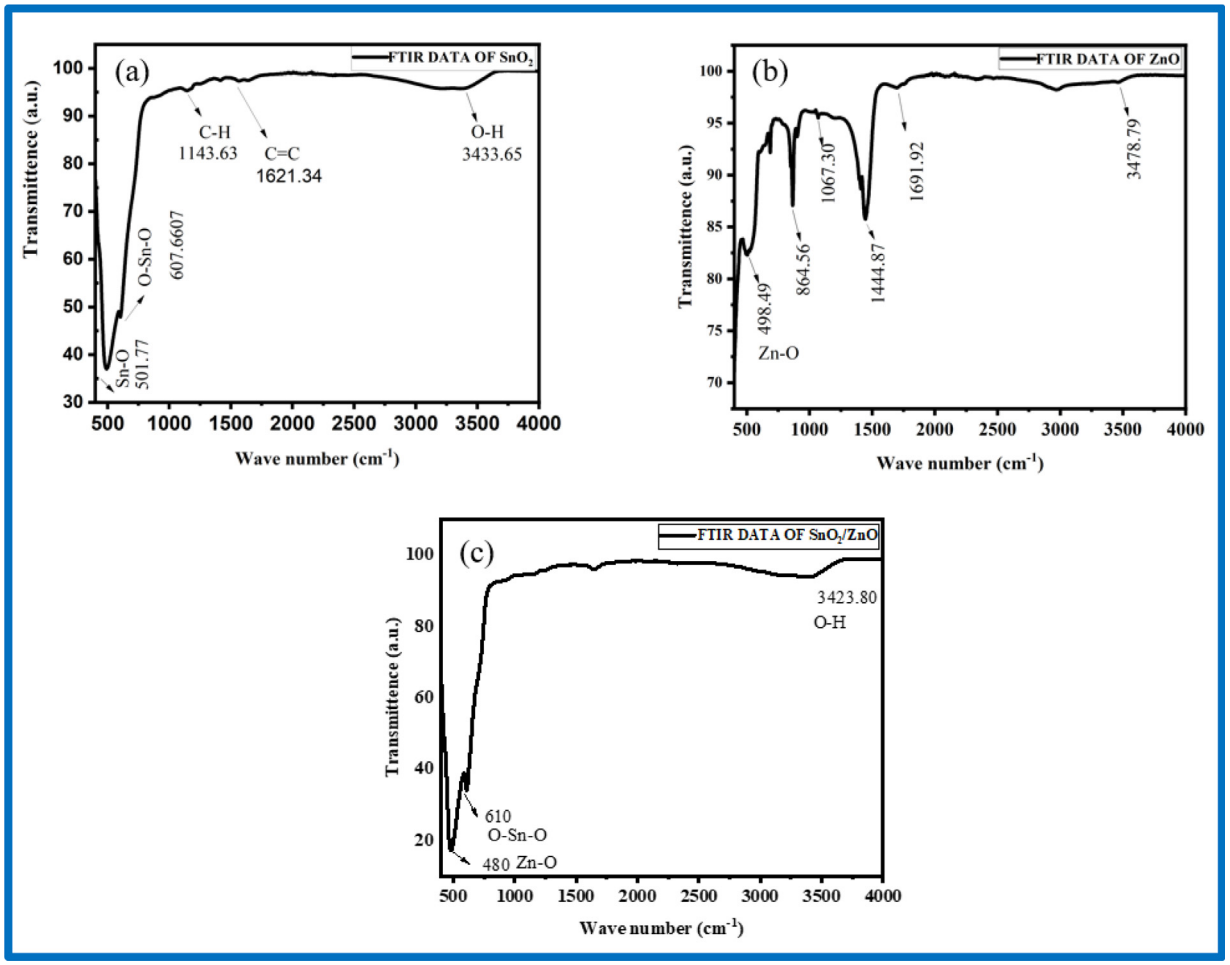

Fig. 6. FTIR graphs of pure SnO_2, ZnO and SnO_2/ZnO composite.

by × and A represents the absorbance, which is a unit less quantity . To obtain the optical band gap of synthesized nanostructures we have plotted the Tauc plot between $(\alpha h\nu)^2$ versus photon energy $(h\nu)$ as shown in Fig. 5 (a-c) by using equation (9).

$$(\alpha h\nu)^2 = A(h\nu - E_g)^n \quad (9)$$

where A is a constant (energy independent),α is the absorption coefficient. E_g represents optical band gap while n is another constant which depends on the type of transition.

To calculate band gap from the Tauc plot an intercept on × axis (energy axis) obtained by extrapolating the linear portion of the Tauc plot. The obtained values for direct band gap of pure SnO_2, ZnO and SnO_2/ZnO composite are 3.68 eV, 3.01 eV and 2.78 eV respectively. The obtained bandgap results are in accordance with the reported literature. SnO_2/ZnO composite have lower direct band gap than pure ZnO and SnO_2. The reduction in bandgap of composite might be because of the generation of new energy levels of ZnO and SnO_2 on formation of composite nanostructure [8][12].

3.4. FTIR analysis

The FTIR spectra of using ATR (Attenuated total reflection) mode, for ZnO, SnO_2, SnO_2/ZnO composites, the FTIR was recorded and various functional groups were obtained which can be confirmed using different absorption peaks as shown in the plots in Fig. 6. Absorbance band around at 607.6 cm^{-1} could be for O-Sn-O, Sn-O lattice which is in accordance with the results obtained by. Further, the absorptions at 3433 cm^{-1} of infrared spectra assigned to hydroxyl groups of water molecules adsorbed on the outer surface of SnO_2 nanorods. Similarly, the absorption peak appearing at 3478 cm^{-1} in the IR spectrum of ZnO nanorods could be assigned to the O-H vibrations, which confirms the presence of hydroxyl (OH) groups on the external surface of ZnO nanorods. Additionally, the appearance of the absorbance band at 498.5 cm^{-1} confirms the formation of ZnO nanorods as reported in literature. The absorbance band at 3423 cm^{-1} appears in the IR spectrum of SnO_2/ZnO composite .

3.5. TEM analysis

The obtained Transmission Electron Microscopic (TEM) images of the synthesized samples are shown in Fig. 7 (a-i) at three different magnifications/scales. It can be observed that the morphology of the synthesized SnO_2, and ZnO are nanobelts and nanorods, respectively. While the nanostructure of SnO_2/ZnO composites is a combination of nanobelts and nanorods as shown in Fig. 7 (g-i). Lattice resolved TEM fringes of surface of the SnO_2, ZnO and SnO_2/ZnO composites are represented in Fig. 8 along with their SAED pattern. The spacing between two neighbouring fringes has been calculated from TEM image (a-c). The obtained average spac-

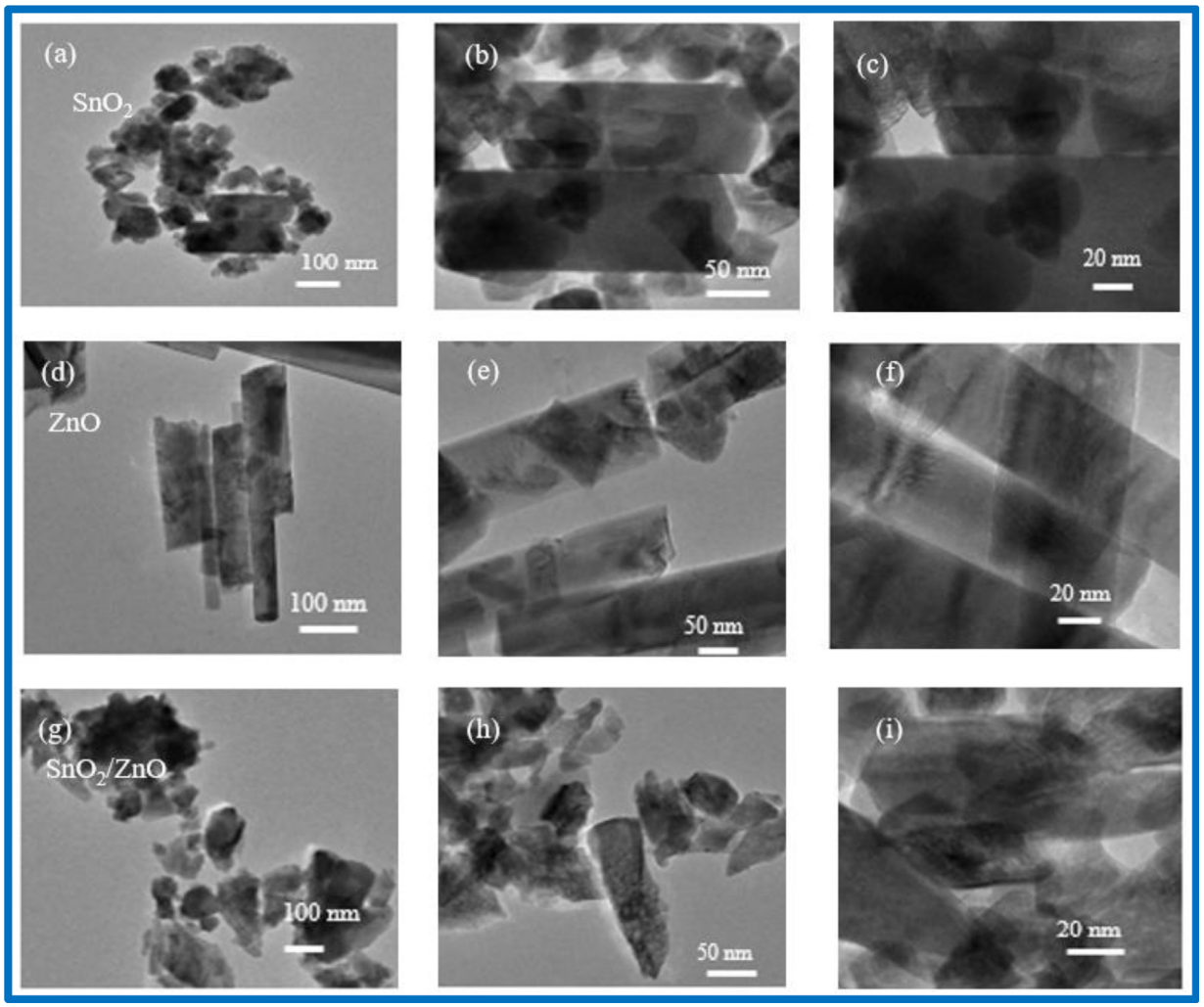

Fig. 7. A typical magnification TEM image of (a-c) SnO2 (d-f) ZnO (g-i) SnO2/ZnO.

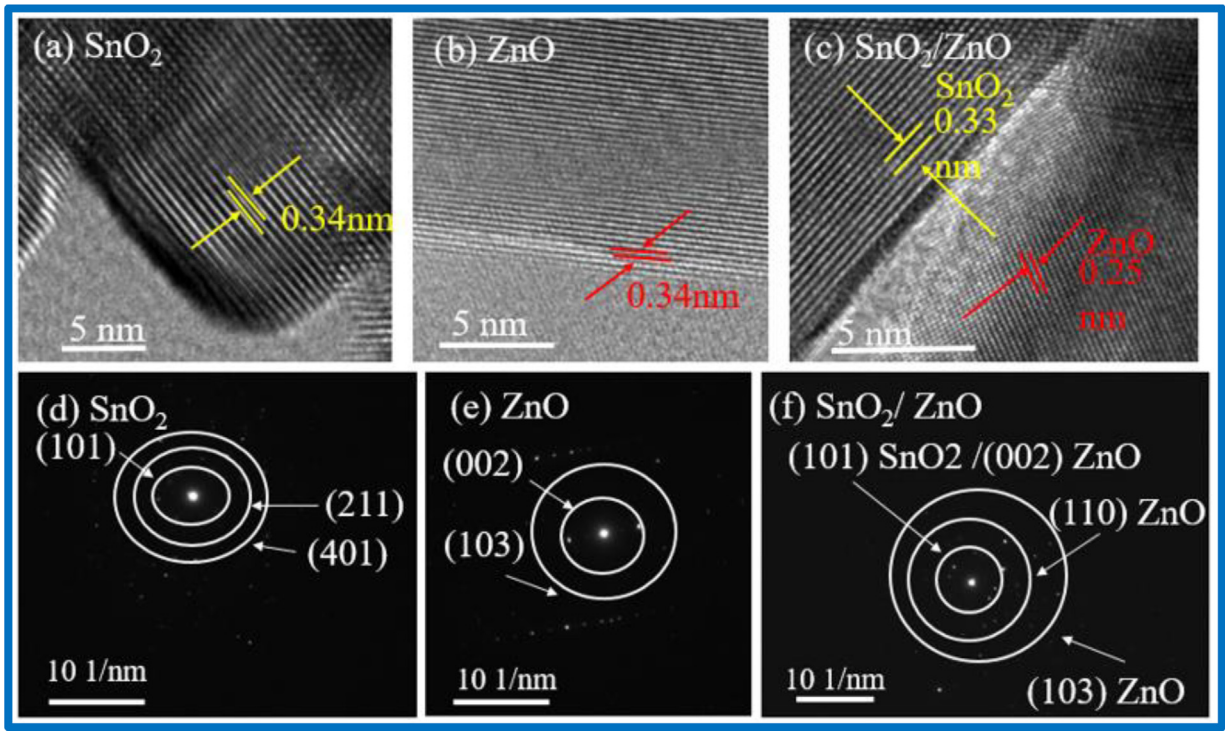

Fig. 8. (a-c) SAED pattern (d-f) Lattice-resolved TEM micrograph of the surface of the SnO_2, ZnO and SnO_2/ZnO composite.

ing for SnO_2 and ZnO fringes are 0.33 nm and 0.25 nm which correspond to (110) of SnO_2 and ZnO (002) crystal planes. The lattice fringes of SnO_2/ZnO composite with average interplanar spacing of 0.33 mm and 0.25 nm are also matched with (110) and (002) planes of SnO2 and ZnO, respectively. This further confirms that the SnO_2/ZnO composite is a two-phase composite material composed of SnO_2 and ZnO.

The SAED, Fig. 8 (d-f), clearly shows the continuous ring diffraction pattern due to the SnO_2 containing a large number of small randomly distributed crystallites for different planes like (101), (211) and (401). ZnO have SAED pattern showing planes (002) and (103). In composite (002) and (101) planes of SnO_2 and ZnO are overlapping with each other while (110) and (103) planes of ZnO are clearly visible [1].

4. Conclusion

Pure SnO_2, ZnO and SnO_2/ZnO composite nanostructures were prepared by using hydrothermal methods. The various structural parameters of synthesized samples were obtained by using Scherrer and W-H Methods. The results indicate that the composites structure has very few additional defects and strain as compared to pure SnO_2 and ZnO. While the observed optical band gap of SnO_2/ZnO composite is smaller than pure SnO_2, and ZnO. Which might be due to generation of new energy levels in the composite structure. The FTIR spectrum further confirms the synthesis of pure SnO_2, pure ZnO and SnO_2/ZnO composites. This study suggests that on synthesis of SnO_2/ZnO composite the structural properties such as phase, lattice strain, defects did not change significantly while the UV–Visible and FTIR absorption peaks get shifted as compared to pure SnO_2 and ZnO. These results are found to be interesting for the application of SnO_2/ZnO composite in the optoelectronic and gas sensing devices.

CRediT authorship contribution statement

Deshraj Meena: Supervision. **Vineeta Yadav:** Conceptualization. **Nirmal Singh:** Conceptualization. **Shilpa Rana:** . **K.M. Komal:** .

Declaration of Competing Interest

The authors declare that they have no known competing financial interests or personal relationships that could have appeared to influence the work reported in this paper.

Reference

[1] J. Guo, J. Zhang, M. Zhu, D. Ju, H. Xu, B. Cao, High-performance gas sensor based on ZnO nanowires functionalized by Au nanoparticles, Sensors Actuators B: Chemical 199 (2014) 339–345.
[2] R.-E. Nowak, M. Vehse, O. Sergeev, T. Voss, M. Seyfried, K. von Maydell, C. Agert, ZnO Nanorods with Broadband Antireflective Properties for Improved Light Management in Silicon Thin-Film Solar Cells, Advanced Optical Materials 2 (1) (2014) 94–99.
[3] N.D. Khoang, D.D. Trung, N. Van Duy, N.D. Hoa, N. Van Hieu, Design of SnO2/ZnO hierarchical nanostructures for enhanced ethanol gas-sensing performance, Sensors and Actuators B: Chemical 174 (2012) 594–601.
[4] Z. Zhang, M. Xu, L. Liu, X. Ruan, J. Yan, W.u. Zhao, J. Yun, Y. Wang, S. Qin, T. Zhang, Novel SnO2@ ZnO hierarchical nanostructures for highly sensitive and selective NO2 gas sensing, Sensors and Actuators B: Chemical 257 (2018) 714–727.
[5] J.-H. Kim et al., Selective H2S sensing without external heat by a synergy effect in self-heated CuO-functionalized SnO2-ZnO core-shell nanowires, Sensors and Actuators B: Chemical 300 (2019) 126981.
[6] W. Zeng, B. Miao, Q.u. Zhou, L. Lin, Hydrothermal synthesis and gas sensing properties of variety low dimensional nanostructures of SnO2, Physica E: Low-dimensional Systems Nanostructures 47 (2013) 116–121.
[7] N.A. Alshehri, A.R. Lewis, C. Pleydell-Pearce, T.G.G. Maffeis, Investigation of the growth parameters of hydrothermal ZnO nanowires for scale up applications, J. Saudi Chemical Society 22 (5) (2018) 538–545.
[8] X. Yang, S. Zhang, Q.i. yu, L. Zhao, P. Sun, T. Wang, F. Liu, X. Yan, Y. Gao, X. Liang, S. Zhang, G. Lu, One step synthesis of branched SnO2/ZnO heterostructures and their enhanced gas-sensing properties, Sensors Actuators B: Chemical 281 (2019) 415–423.

[9] A. Singh, S. Sikarwar, B.C. Yadav, Design and fabrication of quick responsive and highly sensitive LPG sensor using ZnO/SnO2 heterostructured film, Materials Research Express 8 (4) (2021) 045013.

[10] M. Xu et al., Synthesis, growth mechanism, and photoluminescence property of hierarchical SnO 2 nanoflower-rod arrays: An experimental and first principles study. 51 (21) (2016) 9613–9624.

[11] Z. Lu et al., Electrospun ZnO–SnO2 composite nanofibers and enhanced sensing properties to SF6 decomposition byproduct H2S. 6 (2018) 540.

[12] D. Meena, V.K. Verma, S. Rana, Investigation the effect of Zn doping on structural and optical properties of SnO2, Materials Today: Proceedings (2021).